



**SPECKLE NOISE REDUCTION IN ULTRASOUND IMAGE BY
WAVELET THRESHOLDING**

by
TAMILARASAN,P
Reg. No. 1020106018

of

KUMARAGURU COLLEGE OF TECHNOLOGY

(An Autonomous Institution affiliated to Anna University of Technology, Coimbatore)

COIMBATORE - 641049

A PROJECT REPORT

Submitted to the

**FACULTY OF ELECTRONICS AND COMMUNICATION
ENGINEERING**

*In partial fulfillment of the requirements
for the award of the degree*

of

MASTER OF ENGINEERING

in

APPLIED ELECTRONICS

APRIL 2012

BONAFIDE CERTIFICATE

Certified that this project report entitled “**SPECKLE NOISE REDUCTION IN ULTRASOUND IMAGE BY WAVELET THRESHOLDING**” is the bonafide work of **Mr.Tamilarasan,P [Reg. no.1020106018]** who carried out the research under my supervision. Certified further, that to the best of my knowledge the work reported herein does not form part of any other project or dissertation on the basis of which a degree or award was conferred on an earlier occasion on this or any other candidate.

Project Guide

Ms.S.Sasikala

Head of the Department

Dr. Rajeswari Mariappan

The candidate with university Register no. 1020106018 is examined by us in the project viva-voce examination held on

Internal Examiner

External Examiner

ii

ACKNOWLEDGEMENT

First I would like to express my praise and gratitude to the Lord, who has showered his grace and blessing enabling me to complete this project in an excellent manner. He has made all things beautiful in his time.

I express my sincere thanks to our beloved Director **Dr.J.Shanmugam**, Kumaraguru College of Technology, I thank for his kind support and for providing necessary facilities to carry out the work.

I express my sincere thanks to our beloved Principal **Dr.S.Ramachandran**, Kumaraguru College of Technology, who encouraged me in each and every steps of the project work.

I would like to express my sincere thanks and deep sense of gratitude to our HOD, **Dr.Rajeswari Mariappan**, Department of Electronics and Communication Engineering, for her valuable suggestions and encouragement which paved way for the successful completion of the project work. I also thank her for her kind support and for providing necessary facilities to carry out the work.

In particular, I wish to thank and everlasting gratitude to the project coordinator **Ms.R.Hemalatha, M.E.**, Assistant Professor(SRG), Department of Electronics and Communication Engineering for her expert counseling and guidance to make this project to a great deal of success.

I am greatly privileged to express my deep sense of gratitude to my guide **Ms.S.Sasikala, M.Tech.(Ph.d)**, Associate Professor, Department of Electronics and Communication Engineering, Kumaraguru College of Technology throughout the course of this project work and I wish to convey my deep sense of gratitude to all the teaching and non-teaching of ECE Department for their help and cooperation.

Finally, I thank my parents and my family members for giving me the moral support and abundant blessings in all of my activities and my dear friends who helped me to endure my difficult times with their unflinching support and warm wishes.

iii

ABSTRACT

In medical image processing, image denoising has become a very essential exercise all through the diagnose. Arbitration between the perpetuation of useful diagnostic information and noise suppression must be treasured in medical images. In general we rely on the intervention of a proficient to control the quality of processed images. In certain cases, for instance in Ultrasound images, the noise can restrain information which is valuable for the general practitioner. Consequently medical images are very inconsistent, and it is crucial to operate case to case. This project presents a wavelet-based thresholding scheme for noise suppression in ultrasound images. Quantitative and qualitative comparisons of the results obtained by the proposed method with the results achieved from the other speckle noise reduction techniques demonstrate its higher performance for speckle reduction.

iv

TABLE OF CONTENT

CHAPTER NO	TITLE	PAGE NO			PAGE NO
	ABSTRACT	iv	5	WAVELET FILTERING	19
	LIST OF FIGURES	vii		5.1 Wavelet Thresholding	21
	LIST OF TABLES	viii	6	SIMULATION RESULTS	24
1	INTRODUCTION	1	7	CONCLUSION&FUTURE SCOPE	43
	1.1 Project Goal	1			
	1.2 Software Used	1	8	BIBLIOGRAPHY	44
	1.3 Organization Of The Report	2			
2	ULTRASOUND IMAGING SYSTEM	3			
	2.1 Importance Of Ultrasound Image	4			
	2.2 Speckle Noise In Ultrasound Image	5			
3	DESPECKLING FILTERS	6			
	3.1 Filtering Techniques	6			
	3.1.1 Median Filter	6			
	3.1.2 LEE Filter	7			
	3.1.3 Kaun Filter	8			
	3.1.4 SRAD	8			
4	WAVELET	13			
	4.1 Wavelet Definition	13			
	4.1.1 Scaling Filter	13			
	4.1.2 Scaling Function	13			
	4.2 Wavelet Theory	13			
	4.3 Wavelet Transform	14			

v

vi

LIST OF FIGURES

FIGURE NO	CAPTION	PAGE NO
2.1	Block diagram of Ultrasound Imaging System	3
3.1.1.1	Pixel value of image	6
3.1.1.2	Pixel value of Image after Median Filtering	7
3.1.2.1	Flow Chart of LEE Algorithm	8
3.1.4.1	Flow Chart of SRAD Algorithm	12
4.5.1	Types of Wavelets	18
5.1	Decomposition of Wavelets	20
5.1.1	Flow Chart of Wavelet Algorithm	21
6.1	Simulation Result for Breast Image	26
6.2	Simulation Result for Axillary Image	28
6.3	Simulation Result for Fetus Image	29
6.4	Simulation Result for Brain Image	31
6.5	Simulation Result for Heart Image	33
6.6	Simulation Result for Lungs Image	34
6.7	PSNR for Breast Image	38
6.8	PSNR for Axillary Image	38
6.9	PSNR for Fetus Image	39
6.10	PSNR for Brain Image	39
6.11	PSNR for Heart Image	40
6.12	PSNR for Lungs Image	40

vii

LIST OF TABLES

FIGURE NO	CAPTION	PAGE NO
4.5.1	Types Of Wavelets	17
6.1	PSNR for Breast Image	35
6.2	PSNR for Axillary Image	35
6.3	PSNR for Fetus Image	36
6.4	PSNR for Brain Image	36
6.5	PSNR for Heart Image	37
6.6	PSNR for Lungs Image	37
6.7	MSE for Breast Image	41
6.8	MSE for Axillary Image	41
6.9	MSE for Fetus Image	41
6.10	MSE for Brain Image	41
6.11	MSE for Heart Image	41
6.12	MSE for Lungs Image	41
6.13	Threshold Value	42

viii

CHAPTER 1

INTRODUCTION

For the past twenty years, new medical imaging techniques have been under development that image the solid mechanical properties of tissues using pre-existing imaging modalities. An imaging technique involves exposing the object to a form of energy and creating an image from how the object interacts with the input energy. The most popular underlying imaging modality used is ultrasound. Ultrasound imaging is a widely used and safe medical diagnostic technique, due to its noninvasive nature, low cost and capability of forming real time imaging. However the usefulness of ultrasound imaging is degraded by the presence of speckle noise. When structure in the object is too small compared to the wavelength of ultrasound, interference occurs between waves reflected from the object. This produces a mottled appearance in the output image which is termed as speckle noise. The speckle pattern depends on the structure of the image tissue and various imaging parameters. There are two main purposes for speckle reduction in medical ultrasound imaging to improve the human interpretation of ultrasound images and despeckling is the preprocessing step for many ultrasound image processing tasks such as segmentation and registration. A number of methods have been proposed for speckle reduction in ultrasound imaging. While incorporating speckle reduction techniques as an aid for visual diagnosis, it has to keep in mind that certain speckle contains diagnostic information and should be retained. Wavelet based techniques has been used for speckle noise reduction. The results obtained by the wavelets based techniques are compared with other speckle noise reduction techniques to demonstrate its higher performance for speckle noise reduction.

1.1. PROJECT GOAL

The purpose of this project is to reduce speckle noise without losing its significant information in ultrasound images in an efficient way in order to improve the diagnosis.

1.2 SOFTWARES USED

MATLAB R2009a

1

1.3 ORGANIZATION OF THE REPORT

- ✓ Chapter 2 Ultrasound Imaging System.
- ✓ Chapter 3 Despeckling Filters
- ✓ Chapter 4 Wavelets
- ✓ Chapter 5 Wavelet Filtering
- ✓ Chapter 6 Simulation Result
- ✓ Chapter 7 Conclusion
- ✓ Chapter 8 Bibliography

2

CHAPTER 2

ULTRASOUND IMAGING SYSTEM

The construction of ultrasound B-mode image involves capturing the echo signal returned from tissue at the surface of piezoelectric crystal transducers. These transducers convert the ultrasonic RF mechanical wave into electrical signal. Convex ultrasound probes collect the echo from tissue in a radial form. Each group of transducers is simultaneously activated to look at a certain spatial direction from which they generate a raw line signal (stick) to be used later for raster image construction. These sticks are then demodulated and logarithmically compressed to reduce their dynamic range to suit the commercial display devices. The final Cartesian image is constructed from the sampled sticks in a process called scan conversion.

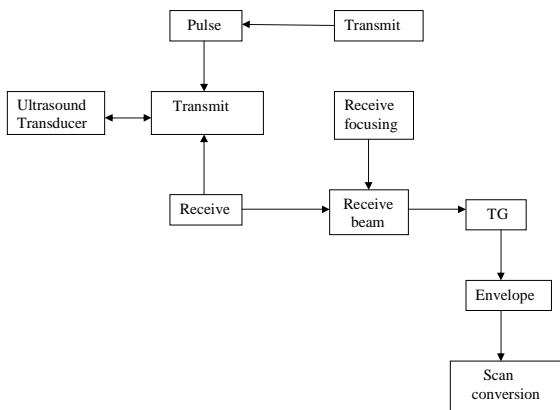


Figure 2.1 Block diagram of Ultrasound Imaging System

3

Speckle reduction techniques can be applied on envelope detected data, log compressed data or on scan converted data. However, slightly different results will be produced for each data. In the compression stage some useful information about the imaged object may be deteriorated or even lost. However, any processing which works with envelope detected data has more information at its disposal and preserves more useful information. Compared to processing the scan converted image, envelope detected data has fewer pixels and thus incurs lower computational cost.

For optimum result envelope detected data processing is preferred because some information that lost after the compression stage cannot be recovered by working with log compressed data or the scan converted image. However, the real time speckle reduction methods are applied on the scan converted image, since the scan converted image is always accessible where most commercial ultrasound systems do not output the envelope detected or log compressed data.

2.1 IMPORTANCE OF ULTRASOUND IMAGING

Ultrasound imaging application in medicine and other fields is enormous. It has several advantages over other medical imaging modalities. The use of ultrasound in diagnosis is well established because of its noninvasive nature, low cost, capability of forming real time imaging and continuing improvement in image quality. It is estimated that one out of every four medical diagnostic image studies in the world involves ultrasonic techniques. US waves are characterized by frequency above 20 KHz which is the upper limit of human hearing. In medical US applications, frequencies are used between 500 KHz and 30 MHz B-mode imaging is the most used modality in medical US. An US transducer which is placed onto the patient's skin over the imaged region sends an US pulse which travels along a beam into the tissue. Due to interfaces some of the US energy is reflected back to the transducer which converts it into echo signals. These signals are then sent into amplifiers and signal processing circuits in the imaging machine's hardware to form a 2-D image. Thus, US imaging involves signals which are obtained by coherent summation of echo signals from scatterers in the tissue. In many cases volume quantification is important in assessing the progression of diseases and tracking progression of response to treatment.

4

Ultrasound-based diagnostic medical imaging technique used to visualize muscles and many internal organs, their size, structure and any pathological injuries with real time tomographic images. It is also used to visualize a fetus during routine and emergency prenatal care. Obstetric sonography is commonly used during pregnancy. It is one of the most widely used diagnostic tools in modern medicine. The technology is relatively inexpensive and portable, especially when compared with other imaging techniques such as magnetic resonance imaging (MRI) and computed tomography (CT). It has no known long-term side effects and rarely causes any discomfort to the patient. Small, easily carried scanners are available examinations can be performed at the bedside. Since it does not use ionizing radiation, ultrasound yields no risks to the patient. It provides live images, where the operator can select the most useful section for diagnosing thus facilitating quick diagnoses. This work aims to suppress speckle in Ultrasound images.

Speckle noise affects all coherent imaging systems including medical ultrasound. Within each resolution cell a number of elementary scatterers reflect the incident wave towards the sensor. The backscattered coherent waves with different phases undergo a constructive or a destructive interference in a random manner. The acquired image is thus corrupted by a random granular pattern, called speckle that delays the interpretation of the image content. A speckled image is commonly modeled as

$$v_i = f_i \xi_i$$

where

$f = \{f_1, f_2, f_3, \dots, f_n\}$ is a noise-free ideal image,

$V = \{v_1, v_2, v_3, \dots, v_n\}$ speckle noise and

$\xi = \{\xi_1, \xi_2, \xi_3, \dots, \xi_n\}$ is a unit mean random field.

The desired grade of speckle smoothing preferably depends on the specialist's knowledge and on the application. For automatic segmentation, sustaining the sharpness of the boundaries between different image regions is usually preferred while smooth out the speckled texture. For visual interpretation, smoothing the texture may be less desirable. Physicians generally have a preference of the original noisy images more willingly than the smoothed versions because the filters even if they are more sophisticated can destroy some relevant image details.

An appropriate method for speckle reduction is one which enhances the signal to noise ratio while preserving the edges and lines in the image. To address the multiplicative nature of speckle noise, Jain developed a homomorphic approach, which is obtained by taking the logarithm of an image, translates the multiplicative noise into additive noise, and consequently applies the Wiener filtering. Recently many techniques have been purposed to reduce the speckle noise using wavelet transform as a multi-resolution image processing tool. Speckle noise is a high-frequency component of the image and appears in wavelet coefficients. One of the widespread method which is mainly exploited for speckle reduction is the wavelet method. A comparative study between wavelet coefficient filter and several standard speckle filters that are being largely used for speckle noise suppression which shows that the wavelet-based approach is deployed among the best for speckle removal.

3.1 FILTERING TECHNIQUES

There are many speckle reduction filters available, some give better visual interpretations while others have good noise reduction or smoothing capabilities. Some of the best known speckle reduction filters are Median, Lee, Kuan and SRAD filters.

3.1.1 MEDIAN FILTER

The Median Filter computes the median of all the pixels within a local window and replaces the center pixel with this median value. Median filtering is a non-linear filtering technique. This method is effective in cases when the noise pattern consists of strong, spike like components and the characteristics to be preserved are edges. The main disadvantage of the median filter is the extra computation time needed to sort the intensity value of each set

15	10	20
23	90	27
33	31	30

Figure 3.1.1.1 Pixel value of image

Sort the pixel value 10 15 20 23 27 30 31 33 90. Find the median 10 15 20 23 27 30 31 33 90

15	10	20
23	27	27
33	31	30

Figure 3.1.1.2 Pixel value of Image after Median Filtering

3.1.2 LEE FILTER

Lee Filter is based on multiplicative speckle model and it can use local statistics to effectively preserve edges. This filter is based on the approach that if the variance over an area is low or constant, then smoothing will not be performed, otherwise smoothing will be performed if variance is high (near edges).

$$Img(i,j) = Im + W * (Cp - Im)$$

Where Img is the pixel Value at indices i, j after filtering, Im is mean intensity of the filter window, Cp is the center pixel and W is a filter window given by:

$$W = \sigma^2 / (\sigma^2 + \rho^2)$$

where σ^2 is the variance of the pixel values within the filter window and is calculated as:

$$\sigma^2 = [1/N \sum_{j=0, N-1} (X_j)^2]$$

Here, N is the size of the filter window and X_j is the pixel value within the filter window at indices j . The parameter ρ is the additive noise variance of the image given in following equation, where M is the size of the image and Y_j is the value of each pixel in the image.

$$\rho^2 = [1/M \sum_{i=0, M-1} (Y_i)^2]$$

If there is no smoothing, the filter will output only the mean intensity value (Im) of the filter window. Otherwise, the difference between Cp and Im is calculated and multiplied with W and then summed with Im . The main drawback of Lee filter is that it tends to ignore speckle noise near edges.

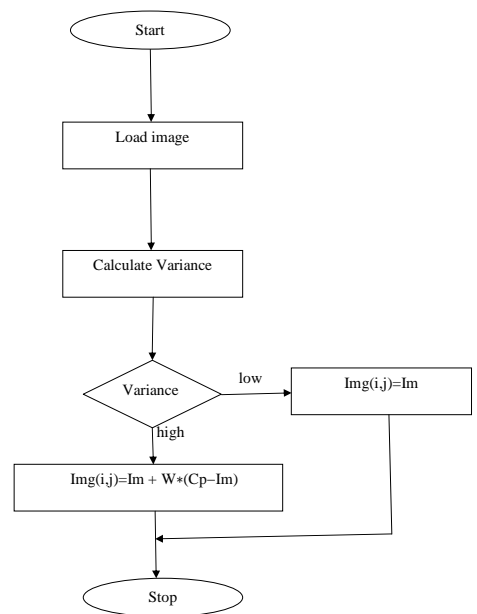


Figure 3.1.2.1 Flow Chart of LEE Algorithm

3.1.3 KAUN FILTER

Kuan filter is a local linear minimum square error filter based on multiplicative order it does not make approximation on the noise variance within the filter window like lee filter it models the multiplicative model of speckle noise into an additive linear form. The weighting function W is computed as follows:

$$W = (1 - Cu/Ci)(1 + Cu)$$

The weighting function is computed from the estimated noise variation coefficient of the image, Cu computed as follows:

$$Cu = \sqrt{1/ENL}$$

And Ci is the variation coefficient of the image computed as follows:

$$Ci = S/Im$$

Where S is the standard deviation in filter window and Im is mean intensity value within the window. The only limitation with Kuan filter is that the ENL parameter is needed for computation.

ENL is Equal Number of Looks which is Calculated as

$$ENL = (\text{Mean Variance}/\text{Standard Deviation})^2$$

3.1.4 SRAD

SRAD stands for Speckle Reduction by Anisotropic Diffusion. In image processing and computer vision, anisotropic diffusion, also called Perona–Malik diffusion, is a technique aiming at reducing image noise without removing significant parts of the image content, typically edges, lines or other details that are important for the interpretation of the image. Anisotropic diffusion resembles the process that creates a scale-space, where an image generates a parameterized family of successively more and more blurred images based on a diffusion process. Each of the

resulting images in this family are given as a convolution between the image and a 2D isotropic Gaussian filter, where the width of the filter increases with the parameter. This diffusion process is a linear and space-invariant transformation of the original image. Anisotropic diffusion is a generalization of this diffusion process: it produces a family of parameterized images, but each resulting image is a combination between the original image and a filter that depends on the local content of the original image. As a consequence, anisotropic diffusion is a non-linear and space-variant transformation of the original image.

In its original formulation, presented by Perona and Malik in 1987, the space-variant filter is in fact isotropic but depends on the image content such that it approximates an impulse function close to edges and other structures that should be preserved in the image over the different levels of the resulting scale-space. This formulation was referred to as anisotropic diffusion by Perona and Malik even though the locally adapted filter is isotropic, but it has also been referred to as inhomogeneous and nonlinear diffusion, or Perona-Malik diffusion. A more general formulation allows the locally adapted filter to be truly anisotropic close to linear structures such as edges or lines: it has an orientation given by the structure such that it is elongated along the structure and narrow across. As a consequence, the resulting images preserve linear structures while at the same time smoothing is made along these structures. Both these cases can be described by a generalization of the usual diffusion equation where the diffusion coefficient, instead of being a constant scalar, is a function of image position and assumes a matrix (or tensor) value.

Although the resulting family of images can be described as a combination between the original image and space-variant filters, the locally adapted filter and its combination with the image do not have to be realized in practice. Anisotropic diffusion is normally implemented by means of an approximation of the generalized diffusion equation: each new image in the family is computed by applying this equation to the previous image. Consequently, anisotropic diffusion is an iterative process where a relatively simple set of computation are used to compute each successive image in the family and this process is continued until a sufficient degree of smoothing is obtained.

SRAD is a Partial Differential Equation (PDE) approach to speckle removal in images. The PDE-based speckle removal approach allows the generation of an image scale space without bias due to filter window size and shape. SRAD is an anisotropic diffusion method for smoothing speckled imagery. Given an intensity image $I_0(x,y)$ having finite power and no zero values over the image support Ω , the output image $I(x, y, t)$ is evolved according to the following PDE:

$$\begin{aligned} \partial I(x,y;t) / \partial t &= \text{div}[c(q)\Delta I(x,y;t)] \\ I(x,y;0) &= I_0(x,y), (\partial I(x,y;t) / \partial n) \partial \Omega = 0 \end{aligned}$$

Where $\partial \Omega$ denotes the border of Ω , n is the outer normal to the $\partial \Omega$, and

$$c(q) = 1 / (1 + q^2(x,y;t) - q_0^2(t) / (q_0^2(t) + q_0^2(t)))$$

$q_0(t)$ is the speckle scale function. In the SRAD, variation $q(x, y, t)$ serves as the edge detector in speckled imagery. The isotropic diffusion in homogenous regions of the image where $q(x, y, t)$ fluctuates around $q_0(t)$. It is estimated using

$$q_0(t) = \text{var}[z(t)] / z(t)$$

where $\text{var}[z(t)]$ and $z(t)$ are the intensity variance and mean over a homogenous area at t , respectively.

3.1.4.1 ALGORITHM

SRAD preserves as well as enhances edges and with the intra region smoothing it reduces speckle noise. In the discrete domain, a gradient can be approximated as the intensity difference between neighboring elements in the image. The filter is iterative $I_0(x,y), (\partial I(x,y;t) / \partial n) \partial \Omega$ describes the change in image intensity produced by one iteration of the filter.

By using the explicit finite difference approach the algorithm for speckle reduction can be designed as the following:

- 1: Design eight 3×3 masks for detecting edges in eight different directions for each pixel of the image.
- 2: for $t = 1$ to n do

- 3: Calculate edges in N,S,E,W,NE,SE,NW,SW directions for each pixel of the image and stored in eight different arrays.
- 4: for all pixels in the image do
- 5: Calculate the value of eight diffusion coefficients for each pixel {Using the elements of the edge arrays}
- 6: Calculate the new intensity of the pixel using the discrete PDE solution.

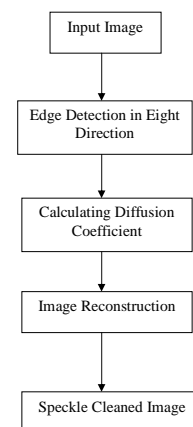


Figure 3.1.4.1 Flow Chart of SRAD Algorithm

CHAPTER 4
WAVELET

4.1 WAVELET DEFINITION

There are a number of ways of defining a wavelet (or a wavelet family).

4.1.1 SCALING FILTER

An orthogonal wavelet is entirely defined by the scaling filter - a low-pass finite impulse response (FIR) filter of length $2N$ and sum 1. In biorthogonal wavelets, separate decomposition and reconstruction filters are defined. For analysis with orthogonal wavelets the high pass filter is calculated as the quadrature mirror filter of the low pass, and reconstruction filters are the time reverse of the decomposition filters. Daubechies and Symlet wavelets can be defined by the scaling filter.

4.1.2 SCALING FUNCTION

Wavelets are defined by the wavelet function $\psi(t)$ (i.e. the mother wavelet) and scaling function $\phi(t)$ (also called father wavelet) in the time domain. The wavelet function is in effect a band-pass filter and scaling it for each level halves its bandwidth. This creates the problem that in order to cover the entire spectrum, an infinite number of levels would be required. The scaling function filters the lowest level of the transform and ensures all the spectrum is covered. For a wavelet with compact support, $\phi(t)$ can be considered finite in length and is equivalent to the scaling filter g . Meyer wavelets can be defined by scaling functions

4.2 WAVELET THEORY

A **wavelet** is a wave-like oscillation with an amplitude that starts out at zero, increases, and then decreases back to zero. It can typically be visualized as a "brief oscillation" like one might see recorded by a seismograph or heart monitor. Generally, wavelets are purposefully crafted to have specific properties that make them useful for signal processing. Wavelets can be

Wavelet transforms are classified into discrete wavelet transforms (DWTs) and continuous wavelet transforms (CWTs). Note that both DWT and CWT are continuous-time (analog) transforms. They can be used to represent continuous-time (analog) signals. CWTs operate over every possible scale and translation whereas DWTs use a specific subset of scale and translation values or representation grid.

4.3.1 CONTINUOUS WAVELET TRANSFORM

In continuous wavelet transforms, a given signal of finite energy is projected on a continuous family of frequency bands (or similar subspaces of the L^2 function space $L^2(\mathbb{R})$).

For instance the signal may be represented on every frequency band of the form $[f^2, f]$ for all positive frequencies $f > 0$. Then, the original signal can be reconstructed by a suitable integration over all the resulting frequency components.

The frequency bands or subspaces (sub-bands) are scaled versions of a subspace at scale I . This subspace in turn is in most situations generated by the shifts of one generating function $\psi \in L^2(\mathbb{R})$, the mother wavelet. For the example of the scale one frequency band $[1, 2]$ this function is

$$\psi(t) = 2 \operatorname{sinc}(2t) - \operatorname{sinc}(t) = \sin(2\pi t) - \sin(\pi t) / \pi$$

4.3.2 DISCRETE WAVELET TRANSFORM

It is computationally impossible to analyze a signal using all wavelet coefficients, so one may wonder if it is sufficient to pick a discrete subset of the upper half plane to be able to reconstruct a signal from the corresponding wavelet coefficients. One such system is the affine system for some real parameters $a > 1, b > 0$. The corresponding discrete subset of the half plane consists of all the points (a^m, na^mb) with integers $m, n \in \mathbb{Z}$. The corresponding *baby wavelets* are now given as

$$\psi_{m,n}(t) = a^{-m/2} \psi(a^{-m}t - nb)$$

A sufficient condition for the reconstruction of any signal x of finite energy by the formula

$$x(t) = \sum_{m \in \mathbb{Z}} \sum_{n \in \mathbb{Z}} \langle x, \psi_{m,n} \rangle \psi_{m,n}(t)$$

combined, using a "revert, shift, multiply and sum" technique called convolution, with portions of an unknown signal to extract information from the unknown signal.

A wavelet could be created to have a frequency of Middle C and a short duration of roughly a 32nd note. If this wavelet were to be convolved at periodic intervals with a signal created from the recording of a song, then the results of these convolutions would be useful for determining when the Middle C note was being played in the song. Mathematically, the wavelet will resonate if the unknown signal contains information of similar frequency - just as a tuning fork physically resonates with sound waves of its specific tuning frequency. This concept of resonance is at the core of many practical applications of wavelet theory. As a mathematical tool, wavelets can be used to extract information from many different kinds of data, including - but certainly not limited to - audio signals and images. Sets of wavelets are generally needed to analyze data fully. A set of "complementary" wavelets will deconstruct data without gaps or overlap so that the deconstruction process is mathematically reversible. Thus, sets of complementary wavelets are useful in wavelet based compression/decompression algorithms where it is desirable to recover the original information with minimal loss. In formal terms, this representation is a wavelet series representation of a square-integrable function with respect to either a complete, orthonormal set of basis functions, or an overcomplete set or frame of a vector space, for the Hilbert space of square integrable functions.

4.3 WAVELET TRANSFORM

A wavelet is a mathematical function used to divide a given function or continuous-time signal into different scale components. Usually one can assign a frequency range to each scale component. Each scale component can then be studied with a resolution that matches its scale. A wavelet transform is the representation of a function by wavelets. The wavelets are scaled and translated copies (known as "daughter wavelets") of a finite-length or fast-decaying oscillating waveform (known as the "mother wavelet"). Wavelet transforms have advantages over traditional Fourier transforms for representing functions that have discontinuities and sharp peaks, and for accurately deconstructing and reconstructing finite, non-periodic and/or non-stationary signals.

is that the functions $\psi_{m,n} : m, n \in \mathbb{Z}$ form a tight frame of $L^2(\mathbb{R})$.

4.4 APPLICATION OF WAVELETS

An approximation to DWT is used for data compression if signal is already sampled, and the CWT for signal analysis. Thus, DWT approximation is commonly used in engineering and computer science, and the CWT in scientific research.

Wavelet transforms are now being adopted for a vast number of applications, often replacing the conventional Fourier Transform. Many areas of physics have seen this paradigm shift, including molecular dynamics, ab initio calculations, astrophysics, density matrix localization, seismology, optics, turbulence, and quantum mechanics. This change has also occurred in image processing, blood-pressure, heart-rate, and ECG analyses, brain rhythms, DNA analysis, protein analysis, climatology, general signal processing, speech recognition, computer graphics and multi fractal analysis. In computer vision and image processing, the notion of scale-space representation and Gaussian derivative operators is regarded as a canonical multi-scale representation.

One use of wavelet approximation is in data compression. Like some other transforms, wavelet transforms can be used to transform data, then encode the transformed data, resulting in effective compression. For example, JPEG 2000 is an image compression standard that uses biorthogonal wavelets. This means that although the frame is overcomplete, it is a *tight frame* (see types of Frame of a vector space), and the same frame functions (except for conjugation in the case of complex wavelets) are used for both analysis and synthesis, i.e., in both the forward and inverse transform. For details see wavelet compression.

A related use is for smoothing/denoising data based on wavelet coefficient thresholding, also called wavelet shrinkage. By adaptively thresholding the wavelet coefficients that correspond to undesired frequency components smoothing and/or denoising operations can be performed.

Wavelet transforms are also starting to be used for communication applications. Wavelet OFDM is the basic modulation scheme used in HD-PLC (a power line communications technology developed by Panasonic), and in one of the optional modes included

in the IEEE 1901 standard. Wavelet OFDM can achieve deeper notches than traditional FFT OFDM, and wavelet OFDM does not require a guard interval (which usually represents significant overhead in FFT OFDM systems).

4.5 TYPES OF WAVELETS

Table 4.5.1 Types of Wavelets

Family Name	Short Name
Haar wavelet	'haar'
Daubechies wavelets	'db'
Symlets	'sym'
Coiflets	'coif'
Biorthogonal wavelets	'bior'
Reverse biorthogonal wavelets	'rbio'
Meyer wavelet	'meyr'
Discrete approximation of Meyer wavelet	'dmey'
Gaussian wavelets	'gaus'
Mexican hat wavelet	'mexh'
Morlet wavelet	'morl'
Complex Gaussian wavelets	'cgau'
Shannon wavelets	'shan'
Frequency B-Spline wavelets	'fbsp'
Complex Morlet wavelets	'cmor'

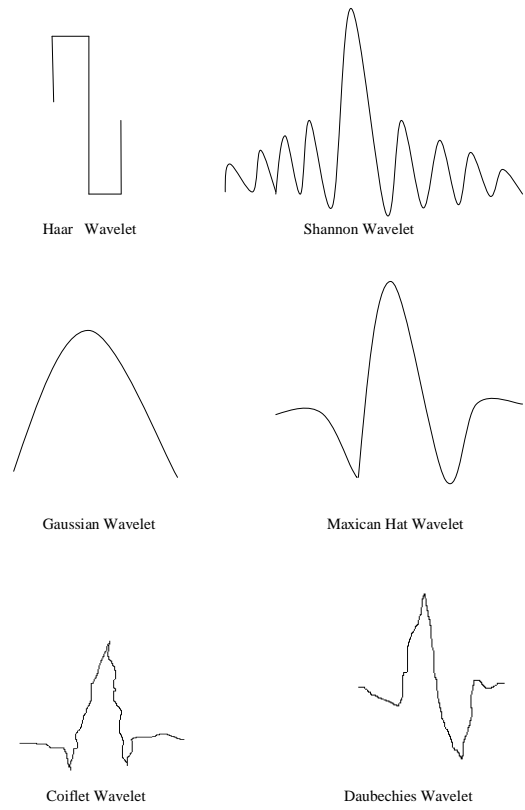


Figure 4.5.1 Types of Wavelets

CHAPTER 5

WAVELET FILTERING

Recently there has been significant investigations in medical imaging area using the wavelet transform as a tool for improving medical images from noisy data. Wavelet denoising attempts to remove the noise present in the signal while preserving the signal characteristics, regardless of its frequency content. As the discrete wavelet transform (DWT) corresponds to basis decomposition, it provides a non redundant and unique representation of the signal.

Several properties of the wavelet transform, which make this representation attractive for denoising, are

- Multiresolution - image details of different sizes are analyzed at the appropriate resolution scales
- Sparsity - the majority of the wavelet coefficients are small in magnitude.
- Edge detection - large wavelet coefficients coincide with image edges.
- Edge clustering - the edge coefficients within each sub band tend to form spatially connected clusters

During a two level of decomposition of an image using a scalar wavelet, the two-dimensional data is replaced with four blocks. These blocks correspond to the sub bands that represent either low pass filtering or high pass filtering in each direction. The procedure for wavelet decomposition consists of consecutive operations on rows and columns of the two-dimensional data. The wavelet transform first performs one step of the transform on all rows. This process yields a matrix where the left side contains down sampled low pass coefficients of each row, and the right side contains the high pass coefficients. Next, one step of decomposition is applied to all columns; this results in four types of coefficients, HH, HL, LH and LL. The HH subband gives the diagonal information of the ultra sound image; the HL subband gives the horizontal features while the LH subband represents the vertical structures of the US image. The LL subband is the low-resolution residual consisting of low frequency components.

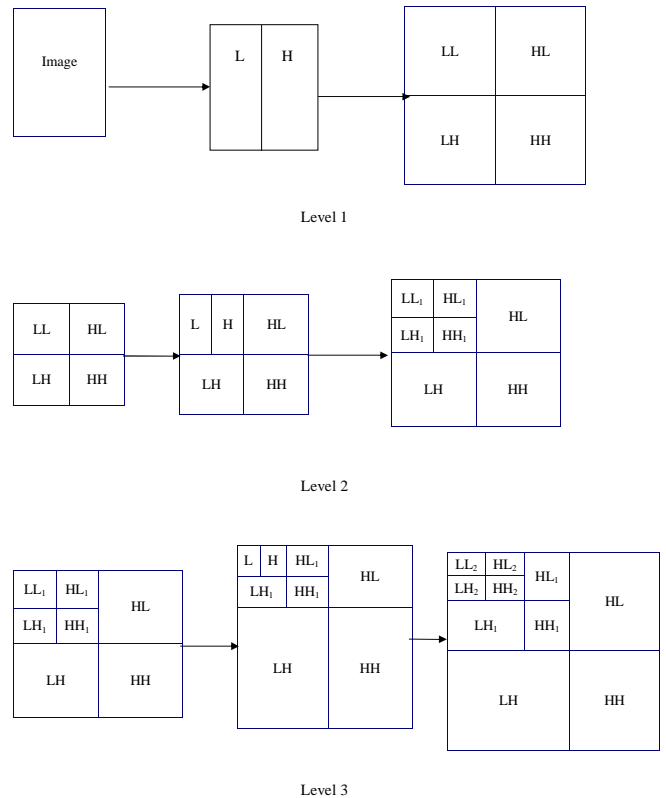


Figure 5.1 Decomposition of Wavelets

5.1 WAVELET THRESHOLDING

All the wavelet filters use wavelet thresholding operation for denoising. Speckle noise is a high-frequency component of the image and appears in wavelet coefficients. One widespread method exploited for speckle reduction is wavelet thresholding procedure. The basic Procedure for all thresholding method is as follows:

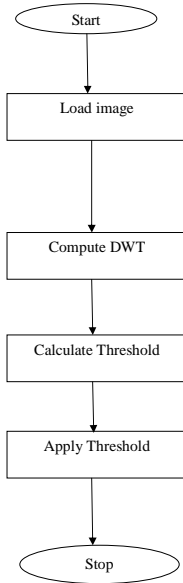


Figure 5.1.1 Flow Chart of Algorithm

21

This section depicts the image-denoising algorithm, which achieves near optimal soft thresholding in the wavelet domain for recovering original signal from the noisy one. The wavelet transform employs Daubechies' least asymmetric compactly supported wavelet with eight vanishing moments with four scales of orthogonal decomposition. It has the following steps.

Transform the multiplicative noise model into an additive one by taking the logarithm of the original speckled data.

- $\text{Log } I(x, y) = \log S(x, y) + \log \eta(x, y)$.
- Perform the DWT of the noisy image
- Obtain noise variance.
- Calculate the weighted variance of image.
- Compute the threshold value for each pixel.
- Perform the inverse DWT to reconstruct the denoised image.
- Take Exponent.

In general a small threshold value will leave behind all the noisy coefficients and subsequently the resultant denoised image may still being noisy. On the other hand a large threshold value makes more number of coefficients as zero which directs to smooth the signal destroys details and the resultant image may cause blur and artifacts. So optimum threshold value should be found out, which is adaptive to different sub band characteristics. Thus the innovative aspects of the present work consist of the estimating appropriate threshold by analyzing the statistical parameters of the wavelet coefficients. Our threshold is based on Universal thresholding function. Threshold is calculated by estimating a parameter weighted variance (δ). The parameter weighted variance (δ) involves neighboring coefficients of the wavelet decomposition for the estimation of the local variance. Weighted variance (δ) of a given wavelet coefficient is determined by the weight in a local window.

$$\delta = \frac{\sum_{i,j \in N} w_{i,j} Y[x,y]^2}{\sum_{i,j \in N} w_{i,j}}$$

22

$Y[x,y]$ is pixel value of the image. w is the weight of the local window. The selection of weights for the calculation of weighted variance would be in such a way that the estimated threshold minimizes the Mean square error.

Threshold (λ) is calculate from noise variance(σ) by weighted variance(δ).

$$\lambda(x, y) = \sigma(x, y) / \delta(x, y)$$

The parameter noise variance (σ) needs to be estimated. It may be possible to measure (σ) based on information other than the corrupted image and it is estimated from the sub band HH by the robust median estimator,

$$\sigma^2(x, y) = [\text{median}/0.6745]^2$$

where 0.6745 is the experimental value.

For quantitative analysis parameters MSE (Mean Square Error), PSNR (peak signal to noise ratio) are calculated for all the standard images with their noisy and denoised counterparts,

$$\text{PSNR} = 10 \log_{10} (255^2 / \text{MSE})$$

$$\text{MSE} = 1 / (M \times N) \sum [X(i,j) - Y(i,j)]^2$$

where X and Y are the original and noisy or denoised image respectively. M and N represent the width and height of image.

23

CHAPTER 6 SIMULATION RESULTS

A program is written and implemented in matlab for denoising the ultrasound images.

MATLAB (matrix laboratory) is a numerical computing environment and fourth-generation programming language. Developed by MathWorks, MATLAB allows matrix manipulations, plotting of functions and data, implementation of algorithms, creation of user interfaces, and interfacing with programs written in other languages, including C, C++, Java, and Fortran.

Key Features

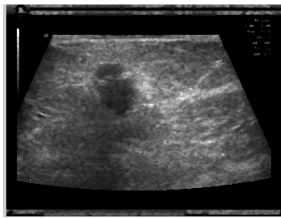
- High-level language for technical computing
- Development environment for managing code, files, and data
- Interactive tools for iterative exploration, design, and problem solving
- Mathematical functions for linear algebra, statistics, Fourier analysis, filtering, optimization, and numerical integration
- 2-D and 3-D graphics functions for visualizing data

The resulting images at various stages of the algorithm for the given input image are shown and attached here.

24



(a) Input Noisy Image



(b) Denoised Image by Median Filter



(c) Denoised Image by Lee Filter



(d) Denoised Image by Kaun Filter



(e) Denoised Image by SRAD



(f) Denoised Image by Wavelet (Haar)



(g) Denoised Image by Wavelet (db2)



(h) Denoised Image by Wavelet (db3)

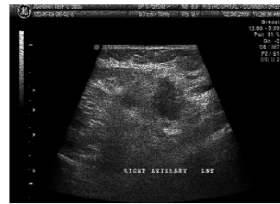


(i) Denoised Image by Wavelet (db4)



(j) Denoised Image by Wavelet (db5)

Figure 6.1 Simulation Results for Breast Image



(a) Input Noisy Image



(b) Denoised Image by Median Filter



(c) Denoised Image by Lee Filter



(d) Denoised Image by Kaun Filter



(i) Denoised Image by Wavelet (db4)



(j) Denoised Image by Wavelet (db5)

Figure 6.2 Simulation Results for Axillary Image



(e) Denoised Image by SRAD



(f) Denoised Image by Wavelet (Haar)



(a) Input Noisy Image



(b) Denoised Image by Median Filter



(g) Denoised Image by Wavelet (db2)



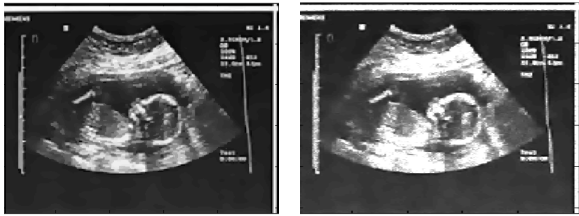
(h) Denoised Image by Wavelet (db3)



(c) Denoised Image by Lee Filter



(d) Denoised Image by Kaun Filter



(e) Denoised Image by SRAD

(f) Denoised Image by Wavelet (Haar)



(g) Denoised Image by Wavelet (db2)



(h) Denoised Image by Wavelet (db3)



(i) Denoised Image by Wavelet (db4)



(j) Denoised Image by Wavelet (db5)

Figure 6.3 Simulation Results for Fetus Image



(a) Input Noisy Image



(b) Denoised Image by Median Filter



(c) Denoised Image by Lee Filter



(d) Denoised Image by Kaun Filter



(e) Denoised Image by SRAD



(f) Denoised Image by Wavelet (Haar)



(g) Denoised Image by Wavelet (db2)



(h) Denoised Image by Wavelet (db3)



(i) Denoised Image by Wavelet (db4)

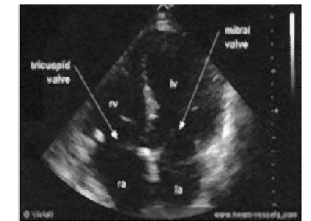


(j) Denoised Image by Wavelet (db5)

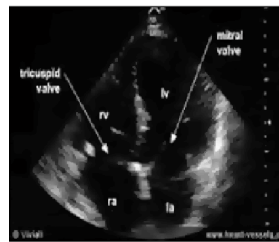
Figure 6.4 Simulation Results for Brain Image



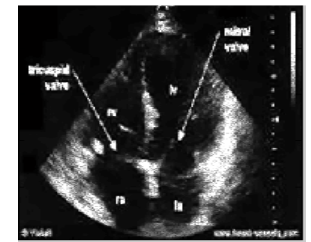
(c) Denoised Image by Lee Filter



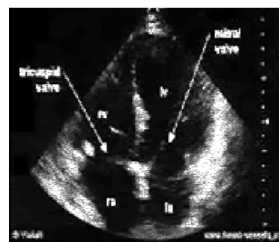
(d) Denoised Image by Kaun Filter



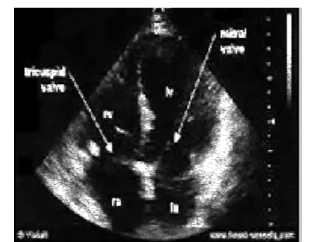
(e) Denoised Image by SRAD



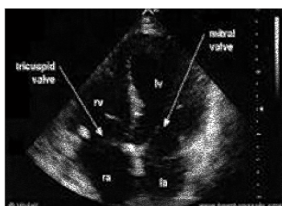
(f) Denoised Image by Wavelet (Haar)



(g) Denoised Image by Wavelet (db2)



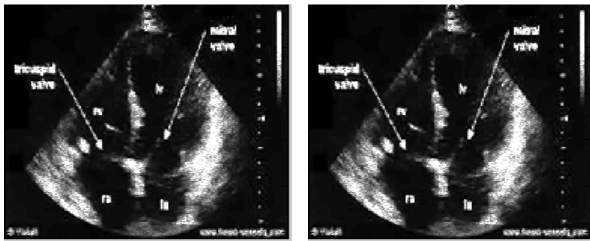
(h) Denoised Image by Wavelet (db3)



(a) Input Noisy Image

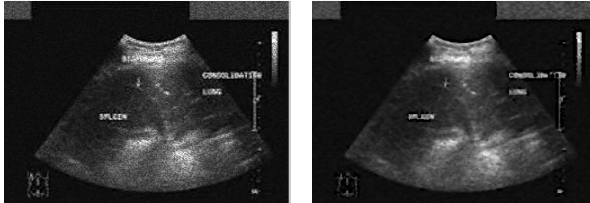


(b) Denoised Image by Median Filter

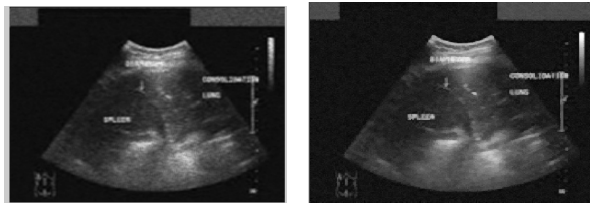


(i) Denoised Image by Wavelet (db4) (j) Denoised Image by Wavelet (db5)

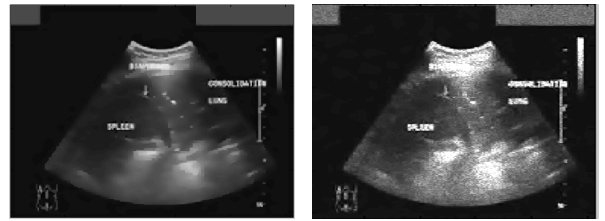
Figure 6.5 Simulation Results for Heart Image



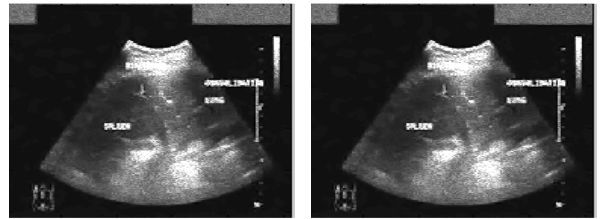
(a) Input Noisy Image (b) Denoised Image by Median Filter



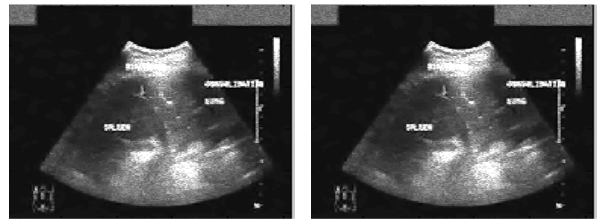
(c) Denoised Image by Lee Filter (d) Denoised Image by Kaun Filter



(e) Denoised Image by SRAD (f) Denoised Image by Wavelet (Haar)



(g) Denoised Image by Wavelet (db2) (h) Denoised Image by Wavelet (db3)



(i) Denoised Image by Wavelet (db4) (j) Denoised Image by Wavelet (db5)

Figure 6.6 Simulation Results for Lungs Image

Table 6.1 PSNR for Breast Image

FILTER	PSNR(db)
MEDIAN	23.7842
LEE	23.6149
KAUN	15.0241
SRAD	23.9094
WAVELET HAAR	24.0654
WAVELET db2	24.0654
WAVELET db3	24.0654
WAVELET db4	24.0654
WAVELET db5	24.0654

Table 6.2 PSNR for Axillary Image

FILTER	PSNR(db)
MEDIAN	23.6949
LEE	23.6063
KAUN	14.9800
SRAD	23.9094
WAVELET HAAR	24.0654
WAVELET db2	24.0654
WAVELET db3	24.0654
WAVELET db4	24.0654
WAVELET db5	24.0654

Table 6.3 PSNR for Fetus Image

FILTER	PSNR(db)
MEDIAN	23.6949
LEE	23.9794
KAUN	14.9792
SRAD	24.0053
WAVELET HAAR	24.0654
WAVELET db2	24.0654
WAVELET db3	24.0654
WAVELET db4	24.0654
WAVELET db5	24.0654

Table 6.4 PSNR for Brain Image

FILTER	PSNR(db)
MEDIAN	23.8445
LEE	23.6922
KAUN	14.9804
SRAD	23.7869
WAVELET HAAR	24.0654
WAVELET db2	24.0654
WAVELET db3	24.0654
WAVELET db4	24.0654
WAVELET db5	24.0654

Table 6.5 PSNR for Heart Image

FILTER	PSNR(db)
MEDIAN	23.7681
LEE	23.9794
KAUN	15.0079
SRAD	24.0042
WAVELET HAAR	24.0654
WAVELET db2	24.0654
WAVELET db3	24.0654
WAVELET db4	24.0654
WAVELET db5	24.0654

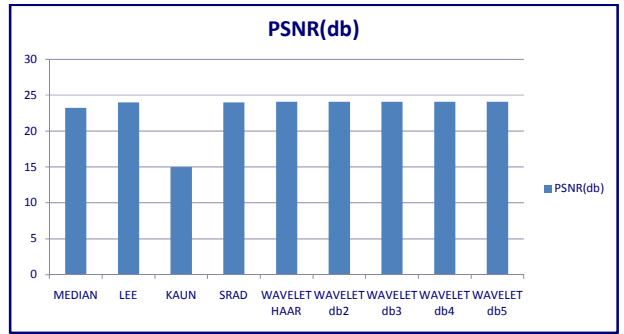


Figure 6.7 PSNR for Breast Image

Table 6.6 PSNR for Lungs Image

FILTER	PSNR(db)
MEDIAN	23.2337
LEE	23.9967
KAUN	14.9883
SRAD	23.9774
WAVELET HAAR	24.0654
WAVELET db2	24.0654
WAVELET db3	24.0654
WAVELET db4	24.0654
WAVELET db5	24.0654

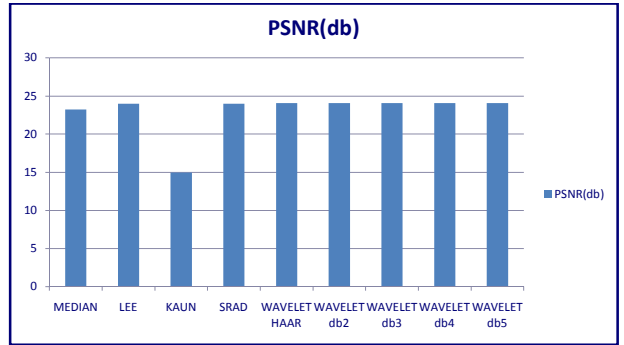


Figure 6.8 PSNR for Axillary Image

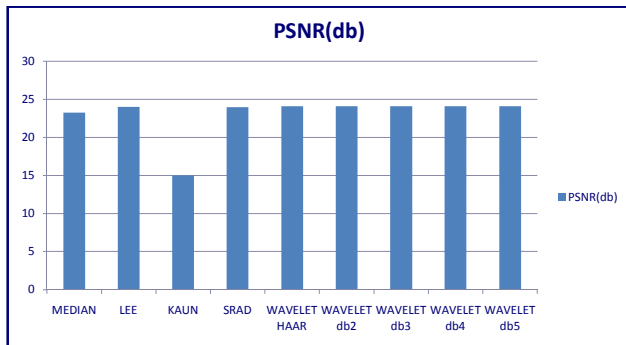


Figure 6.9 PSNR for Fetus Image

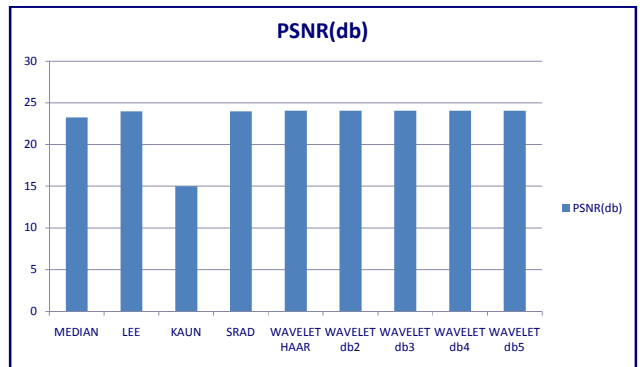


Figure 6.11 PSNR for Heart Image

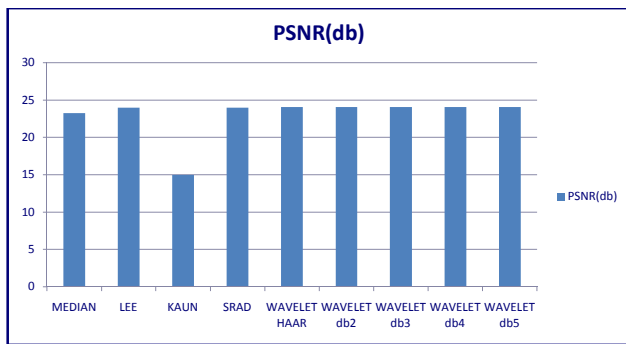


Figure 6.10 PSNR for Brain Image

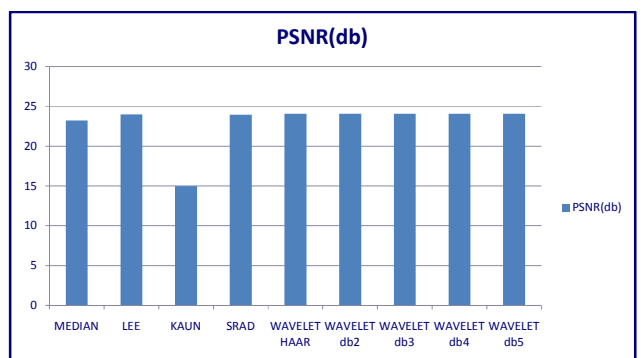


Figure 6.12 PSNR for Lungs Image

Table 6.7 MSE for Breast Image

WAVELET	MSE
HAAR	3.6224
db2	3.5712
db3	3.5674
db4	3.4503
db5	3.5089

Table 6.8 MSE for Axillary Image

WAVELET	MSE
HAAR	0.0421
db2	0.0377
db3	0.0364
db4	0.0355
db5	0.0367

Table 6.9 MSE for Fetus Image

WAVELET	MSE
HAAR	0.8519
db2	0.8022
db3	0.7830
db4	0.7785
db5	0.7824

Table 6.10 MSE for Brain Image

WAVELET	MSE
HAAR	0.1625
db2	0.1654
db3	0.1650
db4	0.1659
db5	0.1711

Table 6.11 MSE for Heart Image

WAVELET	MSE
HAAR	0.5379
db2	0.5058
db3	0.4937
db4	0.4948
db5	0.5056

Table 6.12 MSE for Lungs Image

WAVELET	MSE
HAAR	0.0604
db2	0.0605
db3	0.0616
db4	0.0618
db5	0.0639

Table 6.13 . Threshold Value

IMAGES	TRESHOLD
Breast	3.0976
Axillary	0.3404
Fetus	1.5032
Brain	0.7304
Heart	1.2194
Lungs	0.4359

CHAPTER 7**CONCLUSION & FUTURE SCOPE****Conclusion**

In this work a relatively simple context-based model has been introduced for adaptive threshold selection within a wavelet thresholding framework. Estimations of local weighted variance with appropriately chosen weights are used to adapt the threshold. The proposed thresholding technique outperforms all the standard speckle filters, Median, Lee, Kaun, SRAD methods. However, by visual inspection it is evident that the denoised image, while removing a substantial amount of noise, suffers practically no degradation in sharpness and details. Experimental results show that our proposed method yields significantly improved visual quality as well as better SNR compared to the other techniques in the denoising Techniques.

Future Scope

Multi wavelet may be used to improve the PSNR

CHAPTER 8**BIBLIOGRAPHY**

- [1] Jappret Kaur, Jasdeep Kaur and Manpreet Kaur, "Survey of Despeckling techniques for Medical Ultrasound images", International Journal of Computer Theory and Engineering, Vol 2 (4), 1003-1007, 2011.
- [2] S. Sudha, G.R Suresh and R. Suknesh, "Speckle Noise Reduction in Ultrasound images By Wavelet Thresholding Based On Weighted Variance", International Journal of Computer Theory and Engineering, Vol. 1, No. 1, PP 7-12, 2009.
- [3] S. Sudha, G.R Suresh and R. Suknesh, "Speckle Noise Reduction In ultrasound Images Using Context-Based Adaptive Wavelet Thresholding", IETE Journal of Research Vol 55 (issue 3), 2009.
- [4] Nicolae, M.C., Moraru L., Gogu A., Speckle noise reduction of ultrasound images, Medical Ultrasonography an International Journal of Clinical Imaging, Supplement, 11, 2009, 50-51.
- [5] B. Zhang, J. M. Fadili, and J.-L. Starck "Wavelets, Ridgelets and Curvelets for Poisson Noise Removal" IEEE Transactions on Image Processing, 2007.
- [6] Karl Krissian and Carl Fedrjij "Oriented Speckle reducing anisotropic diffusion", IEEE Trans. Image processing, vol.15, no.5 pp.2694-27014, may 2007
- [7] S.G. Chang, Y. Bin and M. Vetterli: 'Adaptive wavelet thresholding for image denoising and compression', IEEE Trans. On Image Processing, vol.9, no.9, pp. 1532-1546, Sep 2006.
- [8] Yuan Chen, Amar Raheja, "Wavelet Lifting For Speckle Noise Reduction In Ultrasound Images", on Vol.3, pp. 3129- 3132, 17-18, Jan. 2006.

[9] S.Aja-fernandez and C.alberola-lopez,"On the estimation of coefficient of variation for anisotropic diffusion speckle filtering", IEEE Trans. Image processing, vol.15, no.9 pp.2694-27014,Sep.2005

[10] J. S. Lee, "Digital image enhancement and noise filtering by use of local statistics," IEEE Trans.

[11] D. T. Kuan, A. A. Sawchuk, T. C. Strand, and P. Chavel, "Adaptive noise smoothing filter for images with signal-dependent noise," IEEE Trans.



**SPECKLE NOISE REDUCTION IN ULTRASOUND IMAGE BY
WAVELET THRESHOLDING**

by
TAMILARASAN,P
Reg. No. 1020106018

of

KUMARAGURU COLLEGE OF TECHNOLOGY

(An Autonomous Institution affiliated to Anna University of Technology, Coimbatore)

COIMBATORE - 641049

A PROJECT REPORT

Submitted to the

**FACULTY OF ELECTRONICS AND COMMUNICATION
ENGINEERING**

*In partial fulfillment of the requirements
for the award of the degree*

of

MASTER OF ENGINEERING

in

APPLIED ELECTRONICS

APRIL 2012

BONAFIDE CERTIFICATE

Certified that this project report entitled “**SPECKLE NOISE REDUCTION IN ULTRASOUND IMAGE BY WAVELET THRESHOLDING**” is the bonafide work of **Mr.Tamilarasan,P [Reg. no.1020106018]** who carried out the research under my supervision. Certified further, that to the best of my knowledge the work reported herein does not form part of any other project or dissertation on the basis of which a degree or award was conferred on an earlier occasion on this or any other candidate.

Project Guide

Ms.S.Sasikala

Head of the Department

Dr. Rajeswari Mariappan

The candidate with university Register no. 1020106018 is examined by us in the project viva-voce examination held on

Internal Examiner

External Examiner

ii

ACKNOWLEDGEMENT

First I would like to express my praise and gratitude to the Lord, who has showered his grace and blessing enabling me to complete this project in an excellent manner. He has made all things beautiful in his time.

I express my sincere thanks to our beloved Director **Dr.J.Shanmugam**, Kumaraguru College of Technology, I thank for his kind support and for providing necessary facilities to carry out the work.

I express my sincere thanks to our beloved Principal **Dr.S.Ramachandran**, Kumaraguru College of Technology, who encouraged me in each and every steps of the project work.

I would like to express my sincere thanks and deep sense of gratitude to our HOD, **Dr.Rajeswari Mariappan**, Department of Electronics and Communication Engineering, for her valuable suggestions and encouragement which paved way for the successful completion of the project work. I also thank her for her kind support and for providing necessary facilities to carry out the work.

In particular, I wish to thank and everlasting gratitude to the project coordinator **Ms.R.Hemalatha, M.E.**, Assistant Professor(SRG), Department of Electronics and Communication Engineering for her expert counseling and guidance to make this project to a great deal of success.

I am greatly privileged to express my deep sense of gratitude to my guide **Ms.S.Sasikala, M.Tech.(Ph.d)**, Associate Professor, Department of Electronics and Communication Engineering, Kumaraguru College of Technology throughout the course of this project work and I wish to convey my deep sense of gratitude to all the teaching and non-teaching of ECE Department for their help and cooperation.

Finally, I thank my parents and my family members for giving me the moral support and abundant blessings in all of my activities and my dear friends who helped me to endure my difficult times with their unflinching support and warm wishes.

iii

ABSTRACT

In medical image processing, image denoising has become a very essential exercise all through the diagnose. Arbitration between the perpetuation of useful diagnostic information and noise suppression must be treasured in medical images. In general we rely on the intervention of a proficient to control the quality of processed images. In certain cases, for instance in Ultrasound images, the noise can restrain information which is valuable for the general practitioner. Consequently medical images are very inconsistent, and it is crucial to operate case to case. This project presents a wavelet-based thresholding scheme for noise suppression in ultrasound images. Quantitative and qualitative comparisons of the results obtained by the proposed method with the results achieved from the other speckle noise reduction techniques demonstrate its higher performance for speckle reduction.

iv

TABLE OF CONTENT

CHAPTER NO	TITLE	PAGE NO	CHAPTER NO	TITLE	PAGE NO
	ABSTRACT	iv	5	WAVELET FILTERING	19
	LIST OF FIGURES	vii		5.1 Wavelet Thresholding	21
	LIST OF TABLES	viii	6	SIMULATION RESULTS	24
1	INTRODUCTION	1	7	CONCLUSION&FUTURE SCOPE	43
	1.1 Project Goal	1	8	BIBLIOGRAPHY	44
	1.2 Software Used	1			
	1.3 Organization Of The Report	2			
2	ULTRASOUND IMAGING SYSTEM	3			
	2.1 Importance Of Ultrasound Image	4			
	2.2 Speckle Noise In Ultrasound Image	5			
3	DESPECKLING FILTERS	6			
	3.1 Filtering Techniques	6			
	3.1.1 Median Filter	6			
	3.1.2 LEE Filter	7			
	3.1.3 Kaun Filter	8			
	3.1.4 SRAD	8			
4	WAVELET	13			
	4.1 Wavelet Definition	13			
	4.1.1 Scaling Filter	13			
	4.1.2 Scaling Function	13			
	4.2 Wavelet Theory	13			
	4.3 Wavelet Transform	14			

v

vi

LIST OF FIGURES

FIGURE NO	CAPTION	PAGE NO
2.1	Block diagram of Ultrasound Imaging System	3
3.1.1.1	Pixel value of image	6
3.1.1.2	Pixel value of Image after Median Filtering	7
3.1.2.1	Flow Chart of LEE Algorithm	8
3.1.4.1	Flow Chart of SRAD Algorithm	12
4.5.1	Types of Wavelets	18
5.1	Decomposition of Wavelets	20
5.1.1	Flow Chart of Wavelet Algorithm	21
6.1	Simulation Result for Breast Image	26
6.2	Simulation Result for Axillary Image	28
6.3	Simulation Result for Fetus Image	29
6.4	Simulation Result for Brain Image	31
6.5	Simulation Result for Heart Image	33
6.6	Simulation Result for Lungs Image	34
6.7	PSNR for Breast Image	38
6.8	PSNR for Axillary Image	38
6.9	PSNR for Fetus Image	39
6.10	PSNR for Brain Image	39
6.11	PSNR for Heart Image	40
6.12	PSNR for Lungs Image	40

vii

LIST OF TABLES

FIGURE NO	CAPTION	PAGE NO
4.5.1	Types Of Wavelets	17
6.1	PSNR for Breast Image	35
6.2	PSNR for Axillary Image	35
6.3	PSNR for Fetus Image	36
6.4	PSNR for Brain Image	36
6.5	PSNR for Heart Image	37
6.6	PSNR for Lungs Image	37
6.7	MSE for Breast Image	41
6.8	MSE for Axillary Image	41
6.9	MSE for Fetus Image	41
6.10	MSE for Brain Image	41
6.11	MSE for Heart Image	41
6.12	MSE for Lungs Image	41
6.13	Threshold Value	42

viii

CHAPTER 1

INTRODUCTION

For the past twenty years, new medical imaging techniques have been under development that image the solid mechanical properties of tissues using pre-existing imaging modalities. An imaging technique involves exposing the object to a form of energy and creating an image from how the object interacts with the input energy. The most popular underlying imaging modality used is ultrasound. Ultrasound imaging is a widely used and safe medical diagnostic technique, due to its noninvasive nature, low cost and capability of forming real time imaging. However the usefulness of ultrasound imaging is degraded by the presence of speckle noise. When structure in the object is too small compared to the wavelength of ultrasound, interference occurs between waves reflected from the object. This produces a mottled appearance in the output image which is termed as speckle noise. The speckle pattern depends on the structure of the image tissue and various imaging parameters. There are two main purposes for speckle reduction in medical ultrasound imaging to improve the human interpretation of ultrasound images and despeckling is the preprocessing step for many ultrasound image processing tasks such as segmentation and registration. A number of methods have been proposed for speckle reduction in ultrasound imaging. While incorporating speckle reduction techniques as an aid for visual diagnosis, it has to keep in mind that certain speckle contains diagnostic information and should be retained. Wavelet based techniques has been used for speckle noise reduction. The results obtained by the wavelets based techniques are compared with other speckle noise reduction techniques to demonstrate its higher performance for speckle noise reduction.

1.1. PROJECT GOAL

The purpose of this project is to reduce speckle noise without losing its significant information in ultrasound images in an efficient way in order to improve the diagnosis.

1.2 SOFTWARES USED

MATLAB R2009a

1

1.3 ORGANIZATION OF THE REPORT

- ✓ Chapter 2 Ultrasound Imaging System.
- ✓ Chapter 3 Despeckling Filters
- ✓ Chapter 4 Wavelets
- ✓ Chapter 5 Wavelet Filtering
- ✓ Chapter 6 Simulation Result
- ✓ Chapter 7 Conclusion
- ✓ Chapter 8 Bibliography

2

CHAPTER 2

ULTRASOUND IMAGING SYSTEM

The construction of ultrasound B-mode image involves capturing the echo signal returned from tissue at the surface of piezoelectric crystal transducers. These transducers convert the ultrasonic RF mechanical wave into electrical signal. Convex ultrasound probes collect the echo from tissue in a radial form. Each group of transducers is simultaneously activated to look at a certain spatial direction from which they generate a raw line signal (stick) to be used later for raster image construction. These sticks are then demodulated and logarithmically compressed to reduce their dynamic range to suit the commercial display devices. The final Cartesian image is constructed from the sampled sticks in a process called scan conversion.

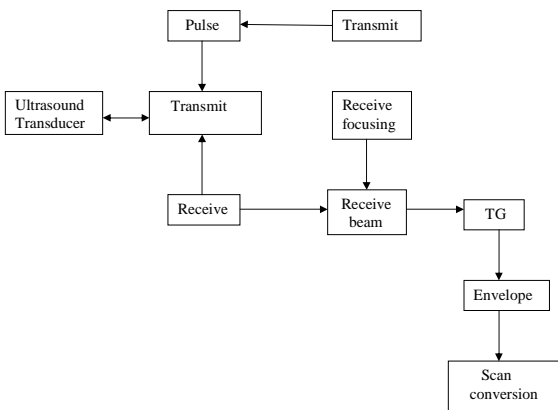


Figure 2.1 Block diagram of Ultrasound Imaging System

3

Speckle reduction techniques can be applied on envelope detected data, log compressed data or on scan converted data. However, slightly different results will be produced for each data. In the compression stage some useful information about the imaged object may be deteriorated or even lost. However, any processing which works with envelope detected data has more information at its disposal and preserves more useful information. Compared to processing the scan converted image, envelope detected data has fewer pixels and thus incurs lower computational cost.

For optimum result envelope detected data processing is preferred because some information that lost after the compression stage cannot be recovered by working with log compressed data or the scan converted image. However, the real time speckle reduction methods are applied on the scan converted image, since the scan converted image is always accessible where most commercial ultrasound systems do not output the envelope detected or log compressed data.

2.1 IMPORTANCE OF ULTRASOUND IMAGING

Ultrasound imaging application in medicine and other fields is enormous. It has several advantages over other medical imaging modalities. The use of ultrasound in diagnosis is well established because of its noninvasive nature, low cost, capability of forming real time imaging and continuing improvement in image quality. It is estimated that one out of every four medical diagnostic image studies in the world involves ultrasonic techniques. US waves are characterized by frequency above 20 KHz which is the upper limit of human hearing. In medical US applications, frequencies are used between 500 KHz and 30 MHz B-mode imaging is the most used modality in medical US. An US transducer which is placed onto the patient's skin over the imaged region sends an US pulse which travels along a beam into the tissue. Due to interfaces some of the US energy is reflected back to the transducer which converts it into echo signals. These signals are then sent into amplifiers and signal processing circuits in the imaging machine's hardware to form a 2-D image. Thus, US imaging involves signals which are obtained by coherent summation of echo signals from scatterers in the tissue. In many cases volume quantification is important in assessing the progression of diseases and tracking progression of response to treatment.

4

Ultrasound-based diagnostic medical imaging technique used to visualize muscles and many internal organs, their size, structure and any pathological injuries with real time tomographic images. It is also used to visualize a fetus during routine and emergency prenatal care. Obstetric sonography is commonly used during pregnancy. It is one of the most widely used diagnostic tools in modern medicine. The technology is relatively inexpensive and portable, especially when compared with other imaging techniques such as magnetic resonance imaging (MRI) and computed tomography (CT). It has no known long-term side effects and rarely causes any discomfort to the patient. Small, easily carried scanners are available examinations can be performed at the bedside. Since it does not use ionizing radiation, ultrasound yields no risks to the patient. It provides live images, where the operator can select the most useful section for diagnosing thus facilitating quick diagnoses. This work aims to suppress speckle in Ultrasound images.

Speckle noise affects all coherent imaging systems including medical ultrasound. Within each resolution cell a number of elementary scatterers reflect the incident wave towards the sensor. The backscattered coherent waves with different phases undergo a constructive or a destructive interference in a random manner. The acquired image is thus corrupted by a random granular pattern, called speckle that delays the interpretation of the image content. A speckled image is commonly modeled as

$$v_i = f_i \xi_i$$

where

$f = \{f_1, f_2, f_3, \dots, f_n\}$ is a noise-free ideal image,

$V = \{v_1, v_2, v_3, \dots, v_n\}$ speckle noise and

$\xi = \{\xi_1, \xi_2, \xi_3, \dots, \xi_n\}$ is a unit mean random field.

The desired grade of speckle smoothing preferably depends on the specialist's knowledge and on the application. For automatic segmentation, sustaining the sharpness of the boundaries between different image regions is usually preferred while smooth out the speckled texture. For visual interpretation, smoothing the texture may be less desirable. Physicians generally have a preference of the original noisy images more willingly than the smoothed versions because the filters even if they are more sophisticated can destroy some relevant image details.

An appropriate method for speckle reduction is one which enhances the signal to noise ratio while preserving the edges and lines in the image. To address the multiplicative nature of speckle noise, Jain developed a homomorphic approach, which is obtained by taking the logarithm of an image, translates the multiplicative noise into additive noise, and consequently applies the Wiener filtering. Recently many techniques have been purposed to reduce the speckle noise using wavelet transform as a multi-resolution image processing tool. Speckle noise is a high-frequency component of the image and appears in wavelet coefficients. One of the widespread method which is mainly exploited for speckle reduction is the wavelet method. A comparative study between wavelet coefficient filter and several standard speckle filters that are being largely used for speckle noise suppression which shows that the wavelet-based approach is deployed among the best for speckle removal.

3.1 FILTERING TECHNIQUES

There are many speckle reduction filters available, some give better visual interpretations while others have good noise reduction or smoothing capabilities. Some of the best known speckle reduction filters are Median, Lee, Kuan and SRAD filters.

3.1.1 MEDIAN FILTER

The Median Filter computes the median of all the pixels within a local window and replaces the center pixel with this median value. Median filtering is a non-linear filtering technique. This method is effective in cases when the noise pattern consists of strong, spike like components and the characteristics to be preserved are edges. The main disadvantage of the median filter is the extra computation time needed to sort the intensity value of each set

15	10	20
23	90	27
33	31	30

Figure 3.1.1.1 Pixel value of image

Sort the pixel value 10 15 20 23 27 30 31 33 90. Find the median 10 15 20 23 27 30 31 33 90

15	10	20
23	27	27
33	31	30

Figure 3.1.1.2 Pixel value of Image after Median Filtering

3.1.2 LEE FILTER

Lee Filter is based on multiplicative speckle model and it can use local statistics to effectively preserve edges. This filter is based on the approach that if the variance over an area is low or constant, then smoothing will not be performed, otherwise smoothing will be performed if variance is high (near edges).

$$Img(i,j) = Im + W * (Cp - Im)$$

Where Img is the pixel Value at indices i, j after filtering, Im is mean intensity of the filter window, Cp is the center pixel and W is a filter window given by:

$$W = \sigma^2 / (\sigma^2 + \rho^2)$$

where σ^2 is the variance of the pixel values within the filter window and is calculated as:

$$\sigma^2 = [1/N \sum_{j=0, N-1} (X_j)^2]$$

Here, N is the size of the filter window and X_j is the pixel value within the filter window at indices j . The parameter ρ is the additive noise variance of the image given in following equation, where M is the size of the image and Y_j is the value of each pixel in the image.

$$\rho^2 = [1/M \sum_{i=0, M-1} (Y_i)^2]$$

If there is no smoothing, the filter will output only the mean intensity value (Im) of the filter window. Otherwise, the difference between Cp and Im is calculated and multiplied with W and then summed with Im . The main drawback of Lee filter is that it tends to ignore speckle noise near edges.

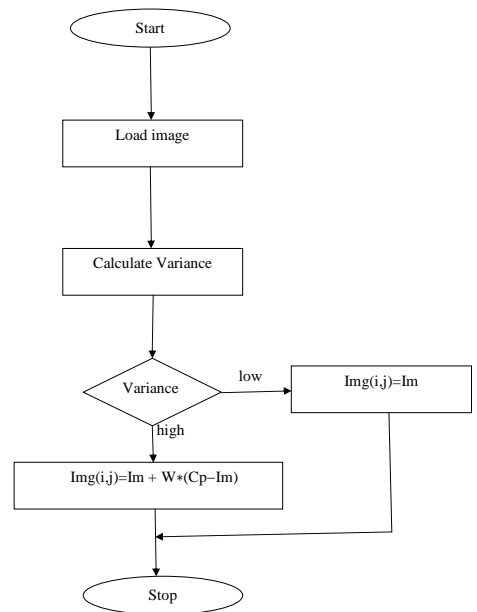


Figure 3.1.2.1 Flow Chart of LEE Algorithm

3.1.3 KAUN FILTER

Kuan filter is a local linear minimum square error filter based on multiplicative order it does not make approximation on the noise variance within the filter window like lee filter it models the multiplicative model of speckle noise into an additive linear form. The weighting function W is computed as follows:

$$W = (1 - Cu/Ci)(1 + Cu)$$

The weighting function is computed from the estimated noise variation coefficient of the image, Cu computed as follows:

$$Cu = \sqrt{1/ENL}$$

And Ci is the variation coefficient of the image computed as follows:

$$Ci = S/Im$$

Where S is the standard deviation in filter window and Im is mean intensity value within the window. The only limitation with Kuan filter is that the ENL parameter is needed for computation.

ENL is Equal Number of Looks which is Calculated as

$$ENL = (\text{Mean Variance}/\text{Standard Deviation})^2$$

3.1.4 SRAD

SRAD stands for Speckle Reduction by Anisotropic Diffusion. In image processing and computer vision, anisotropic diffusion, also called Perona–Malik diffusion, is a technique aiming at reducing image noise without removing significant parts of the image content, typically edges, lines or other details that are important for the interpretation of the image. Anisotropic diffusion resembles the process that creates a scale-space, where an image generates a parameterized family of successively more and more blurred images based on a diffusion process. Each of the

resulting images in this family are given as a convolution between the image and a 2D isotropic Gaussian filter, where the width of the filter increases with the parameter. This diffusion process is a linear and space-invariant transformation of the original image. Anisotropic diffusion is a generalization of this diffusion process: it produces a family of parameterized images, but each resulting image is a combination between the original image and a filter that depends on the local content of the original image. As a consequence, anisotropic diffusion is a non-linear and space-variant transformation of the original image.

In its original formulation, presented by Perona and Malik in 1987, the space-variant filter is in fact isotropic but depends on the image content such that it approximates an impulse function close to edges and other structures that should be preserved in the image over the different levels of the resulting scale-space. This formulation was referred to as anisotropic diffusion by Perona and Malik even though the locally adapted filter is isotropic, but it has also been referred to as inhomogeneous and nonlinear diffusion, or Perona-Malik diffusion. A more general formulation allows the locally adapted filter to be truly anisotropic close to linear structures such as edges or lines: it has an orientation given by the structure such that it is elongated along the structure and narrow across. As a consequence, the resulting images preserve linear structures while at the same time smoothing is made along these structures. Both these cases can be described by a generalization of the usual diffusion equation where the diffusion coefficient, instead of being a constant scalar, is a function of image position and assumes a matrix (or tensor) value.

Although the resulting family of images can be described as a combination between the original image and space-variant filters, the locally adapted filter and its combination with the image do not have to be realized in practice. Anisotropic diffusion is normally implemented by means of an approximation of the generalized diffusion equation: each new image in the family is computed by applying this equation to the previous image. Consequently, anisotropic diffusion is an iterative process where a relatively simple set of computation are used to compute each successive image in the family and this process is continued until a sufficient degree of smoothing is obtained.

SRAD is a Partial Differential Equation (PDE) approach to speckle removal in images. The PDE-based speckle removal approach allows the generation of an image scale space without bias due to filter window size and shape. SRAD is an anisotropic diffusion method for smoothing speckled imagery. Given an intensity image $I_0(x,y)$ having finite power and no zero values over the image support Ω , the output image $I(x, y, t)$ is evolved according to the following PDE:

$$\begin{aligned} \partial I(x,y;t) / \partial t &= \text{div}[c(q)\Delta I(x,y;t)] \\ I(x,y;0) &= I_0(x,y), (\partial I(x,y;t) / \partial n) \partial \Omega = 0 \end{aligned}$$

Where $\partial \Omega$ denotes the border of Ω , n is the outer normal to the $\partial \Omega$, and

$$c(q) = 1 / (1 + q^2(x,y;t) - q_0^2(t) / (q_0^2(t) + q_0^2(t)))$$

$q_0(t)$ is the speckle scale function. In the SRAD, variation $q(x, y, t)$ serves as the edge detector in speckled imagery. The isotropic diffusion in homogenous regions of the image where $q(x, y, t)$ fluctuates around $q_0(t)$. It is estimated using

$$q_0(t) = \text{var}[z(t)] / z(t)$$

where $\text{var}[z(t)]$ and $z(t)$ are the intensity variance and mean over a homogenous area at t , respectively.

3.1.4.1 ALGORITHM

SRAD preserves as well as enhances edges and with the intra region smoothing it reduces speckle noise. In the discrete domain, a gradient can be approximated as the intensity difference between neighboring elements in the image. The filter is iterative $I_0(x,y), (\partial I(x,y;t) / \partial n) \partial \Omega$ describes the change in image intensity produced by one iteration of the filter.

By using the explicit finite difference approach the algorithm for speckle reduction can be designed as the following:

- 1: Design eight 3×3 masks for detecting edges in eight different directions for each pixel of the image.
- 2: for $t = 1$ to n do

- 3: Calculate edges in N,S,E,W,NE,SE,NW,SW directions for each pixel of the image and stored in eight different arrays.
- 4: for all pixels in the image do
- 5: Calculate the value of eight diffusion coefficients for each pixel {Using the elements of the edge arrays}
- 6: Calculate the new intensity of the pixel using the discrete PDE solution.

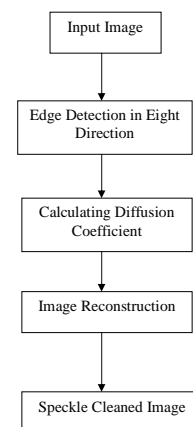


Figure 3.1.4.1 Flow Chart of SRAD Algorithm

CHAPTER 4
WAVELET

4.1 WAVELET DEFINITION

There are a number of ways of defining a wavelet (or a wavelet family).

4.1.1 SCALING FILTER

An orthogonal wavelet is entirely defined by the scaling filter - a low-pass finite impulse response (FIR) filter of length $2N$ and sum 1. In biorthogonal wavelets, separate decomposition and reconstruction filters are defined. For analysis with orthogonal wavelets the high pass filter is calculated as the quadrature mirror filter of the low pass, and reconstruction filters are the time reverse of the decomposition filters. Daubechies and Symlet wavelets can be defined by the scaling filter.

4.1.2 SCALING FUNCTION

Wavelets are defined by the wavelet function $\psi(t)$ (i.e. the mother wavelet) and scaling function $\phi(t)$ (also called father wavelet) in the time domain. The wavelet function is in effect a band-pass filter and scaling it for each level halves its bandwidth. This creates the problem that in order to cover the entire spectrum, an infinite number of levels would be required. The scaling function filters the lowest level of the transform and ensures all the spectrum is covered. For a wavelet with compact support, $\phi(t)$ can be considered finite in length and is equivalent to the scaling filter g . Meyer wavelets can be defined by scaling functions

4.2 WAVELET THEORY

A wavelet is a wave-like oscillation with an amplitude that starts out at zero, increases, and then decreases back to zero. It can typically be visualized as a "brief oscillation" like one might see recorded by a seismograph or heart monitor. Generally, wavelets are purposefully crafted to have specific properties that make them useful for signal processing. Wavelets can be

Wavelet transforms are classified into discrete wavelet transforms (DWTs) and continuous wavelet transforms (CWTs). Note that both DWT and CWT are continuous-time (analog) transforms. They can be used to represent continuous-time (analog) signals. CWTs operate over every possible scale and translation whereas DWTs use a specific subset of scale and translation values or representation grid.

4.3.1 CONTINUOUS WAVELET TRANSFORM

In continuous wavelet transforms, a given signal of finite energy is projected on a continuous family of frequency bands (or similar subspaces of the L^2 function space $L^2(\mathbb{R})$).

For instance the signal may be represented on every frequency band of the form $[f^2, f]$ for all positive frequencies $f > 0$. Then, the original signal can be reconstructed by a suitable integration over all the resulting frequency components.

The frequency bands or subspaces (sub-bands) are scaled versions of a subspace at scale I . This subspace in turn is in most situations generated by the shifts of one generating function $\psi \in L^2(\mathbb{R})$, the mother wavelet. For the example of the scale one frequency band $[1, 2]$ this function is

$$\psi(t) = 2 \operatorname{sinc}(2t) - \operatorname{sinc}(t) = \sin(2\pi t) - \sin(\pi t) / \pi$$

4.3.2 DISCRETE WAVELET TRANSFORM

It is computationally impossible to analyze a signal using all wavelet coefficients, so one may wonder if it is sufficient to pick a discrete subset of the upper half plane to be able to reconstruct a signal from the corresponding wavelet coefficients. One such system is the affine system for some real parameters $a > 1, b > 0$. The corresponding discrete subset of the half plane consists of all the points (a^m, na^mb) with integers $m, n \in \mathbb{Z}$. The corresponding baby wavelets are now given as

$$\psi_{m,n}(t) = a^{-m/2} \psi(a^{-m}t - nb)$$

A sufficient condition for the reconstruction of any signal x of finite energy by the formula

$$x(t) = \sum_{m \in \mathbb{Z}} \sum_{n \in \mathbb{Z}} \langle x, \psi_{m,n} \rangle \psi_{m,n}(t)$$

combined, using a "revert, shift, multiply and sum" technique called convolution, with portions of an unknown signal to extract information from the unknown signal.

A wavelet could be created to have a frequency of Middle C and a short duration of roughly a 32nd note. If this wavelet were to be convolved at periodic intervals with a signal created from the recording of a song, then the results of these convolutions would be useful for determining when the Middle C note was being played in the song. Mathematically, the wavelet will resonate if the unknown signal contains information of similar frequency - just as a tuning fork physically resonates with sound waves of its specific tuning frequency. This concept of resonance is at the core of many practical applications of wavelet theory. As a mathematical tool, wavelets can be used to extract information from many different kinds of data, including - but certainly not limited to - audio signals and images. Sets of wavelets are generally needed to analyze data fully. A set of "complementary" wavelets will deconstruct data without gaps or overlap so that the deconstruction process is mathematically reversible. Thus, sets of complementary wavelets are useful in wavelet based compression/decompression algorithms where it is desirable to recover the original information with minimal loss. In formal terms, this representation is a wavelet series representation of a square-integrable function with respect to either a complete, orthonormal set of basis functions, or an overcomplete set or frame of a vector space, for the Hilbert space of square integrable functions.

4.3 WAVELET TRANSFORM

A wavelet is a mathematical function used to divide a given function or continuous-time signal into different scale components. Usually one can assign a frequency range to each scale component. Each scale component can then be studied with a resolution that matches its scale. A wavelet transform is the representation of a function by wavelets. The wavelets are scaled and translated copies (known as "daughter wavelets") of a finite-length or fast-decaying oscillating waveform (known as the "mother wavelet"). Wavelet transforms have advantages over traditional Fourier transforms for representing functions that have discontinuities and sharp peaks, and for accurately deconstructing and reconstructing finite, non-periodic and/or non-stationary signals.

is that the functions $\psi_{m,n} : m, n \in \mathbb{Z}$ form a tight frame of $L^2(\mathbb{R})$.

4.4 APPLICATION OF WAVELETS

An approximation to DWT is used for data compression if signal is already sampled, and the CWT for signal analysis. Thus, DWT approximation is commonly used in engineering and computer science, and the CWT in scientific research.

Wavelet transforms are now being adopted for a vast number of applications, often replacing the conventional Fourier Transform. Many areas of physics have seen this paradigm shift, including molecular dynamics, ab initio calculations, astrophysics, density matrix localization, seismology, optics, turbulence, and quantum mechanics. This change has also occurred in image processing, blood-pressure, heart-rate, and ECG analyses, brain rhythms, DNA analysis, protein analysis, climatology, general signal processing, speech recognition, computer graphics and multi fractal analysis. In computer vision and image processing, the notion of scale-space representation and Gaussian derivative operators is regarded as a canonical multi-scale representation.

One use of wavelet approximation is in data compression. Like some other transforms, wavelet transforms can be used to transform data, then encode the transformed data, resulting in effective compression. For example, JPEG 2000 is an image compression standard that uses biorthogonal wavelets. This means that although the frame is overcomplete, it is a *tight frame* (see types of Frame of a vector space), and the same frame functions (except for conjugation in the case of complex wavelets) are used for both analysis and synthesis, i.e., in both the forward and inverse transform. For details see wavelet compression.

A related use is for smoothing/denoising data based on wavelet coefficient thresholding, also called wavelet shrinkage. By adaptively thresholding the wavelet coefficients that correspond to undesired frequency components smoothing and/or denoising operations can be performed.

Wavelet transforms are also starting to be used for communication applications. Wavelet OFDM is the basic modulation scheme used in HD-PLC (a power line communications technology developed by Panasonic), and in one of the optional modes included

in the IEEE 1901 standard. Wavelet OFDM can achieve deeper notches than traditional FFT OFDM, and wavelet OFDM does not require a guard interval (which usually represents significant overhead in FFT OFDM systems).

4.5 TYPES OF WAVELETS

Table 4.5.1 Types of Wavelets

Family Name	Short Name
Haar wavelet	'haar'
Daubechies wavelets	'db'
Symlets	'sym'
Coiflets	'coif'
Biorthogonal wavelets	'bior'
Reverse biorthogonal wavelets	'rbio'
Meyer wavelet	'meyr'
Discrete approximation of Meyer wavelet	'dmey'
Gaussian wavelets	'gaus'
Mexican hat wavelet	'mexh'
Morlet wavelet	'morl'
Complex Gaussian wavelets	'cgau'
Shannon wavelets	'shan'
Frequency B-Spline wavelets	'fbsp'
Complex Morlet wavelets	'cmor'

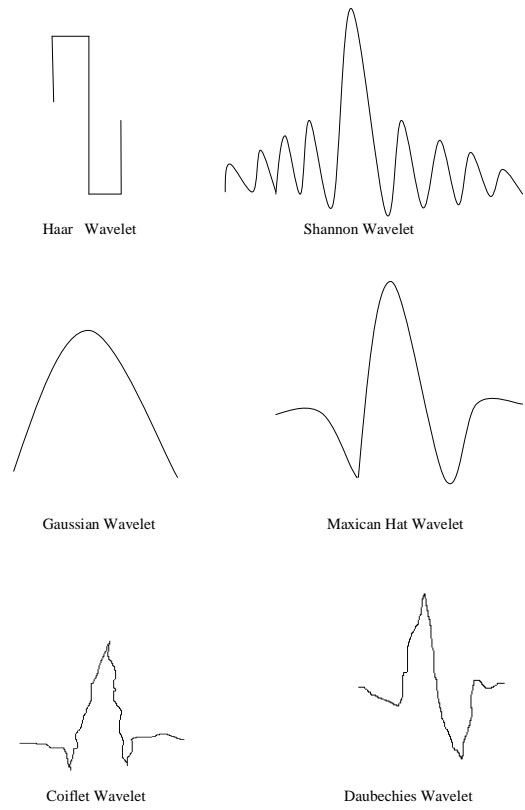


Figure 4.5.1 Types of Wavelets

CHAPTER 5

WAVELET FILTERING

Recently there has been significant investigations in medical imaging area using the wavelet transform as a tool for improving medical images from noisy data. Wavelet denoising attempts to remove the noise present in the signal while preserving the signal characteristics, regardless of its frequency content. As the discrete wavelet transform (DWT) corresponds to basis decomposition, it provides a non redundant and unique representation of the signal.

Several properties of the wavelet transform, which make this representation attractive for denoising, are

- Multiresolution - image details of different sizes are analyzed at the appropriate resolution scales
- Sparsity - the majority of the wavelet coefficients are small in magnitude.
- Edge detection - large wavelet coefficients coincide with image edges.
- Edge clustering - the edge coefficients within each sub band tend to form spatially connected clusters

During a two level of decomposition of an image using a scalar wavelet, the two-dimensional data is replaced with four blocks. These blocks correspond to the sub bands that represent either low pass filtering or high pass filtering in each direction. The procedure for wavelet decomposition consists of consecutive operations on rows and columns of the two-dimensional data. The wavelet transform first performs one step of the transform on all rows. This process yields a matrix where the left side contains down sampled low pass coefficients of each row, and the right side contains the high pass coefficients. Next, one step of decomposition is applied to all columns; this results in four types of coefficients, HH, HL, LH and LL. The HH subband gives the diagonal information of the ultra sound image; the HL subband gives the horizontal features while the LH subband represents the vertical structures of the US image. The LL subband is the low-resolution residual consisting of low frequency components.

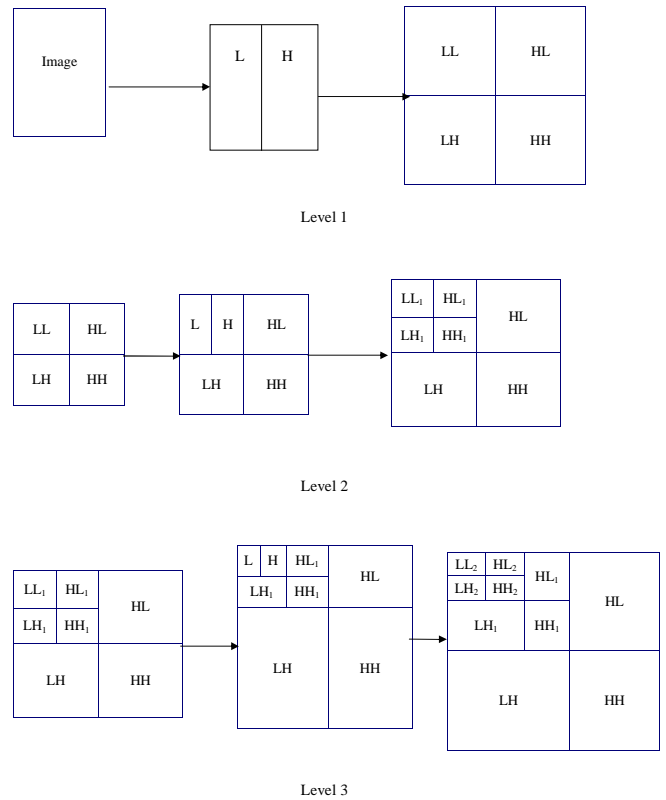


Figure 5.1 Decomposition of Wavelets

5.1 WAVELET THRESHOLDING

All the wavelet filters use wavelet thresholding operation for denoising. Speckle noise is a high-frequency component of the image and appears in wavelet coefficients. One widespread method exploited for speckle reduction is wavelet thresholding procedure. The basic Procedure for all thresholding method is as follows:

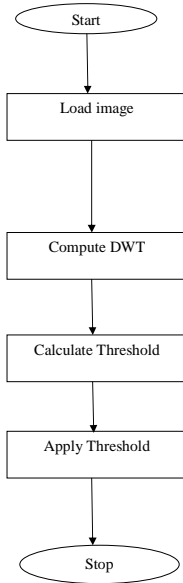


Figure 5.1.1 Flow Chart of Algorithm

21

This section depicts the image-denoising algorithm, which achieves near optimal soft thresholding in the wavelet domain for recovering original signal from the noisy one. The wavelet transform employs Daubechies' least asymmetric compactly supported wavelet with eight vanishing moments with four scales of orthogonal decomposition. It has the following steps.

Transform the multiplicative noise model into an additive one by taking the logarithm of the original speckled data.

- $\text{Log } I(x, y) = \log S(x, y) + \log \eta(x, y)$.
- Perform the DWT of the noisy image
- Obtain noise variance.
- Calculate the weighted variance of image.
- Compute the threshold value for each pixel.
- Perform the inverse DWT to reconstruct the denoised image.
- Take Exponent.

In general a small threshold value will leave behind all the noisy coefficients and subsequently the resultant denoised image may still being noisy. On the other hand a large threshold value makes more number of coefficients as zero which directs to smooth the signal destroys details and the resultant image may cause blur and artifacts. So optimum threshold value should be found out, which is adaptive to different sub band characteristics. Thus the innovative aspects of the present work consist of the estimating appropriate threshold by analyzing the statistical parameters of the wavelet coefficients. Our threshold is based on Universal thresholding function. Threshold is calculated by estimating a parameter weighted variance (δ). The parameter weighted variance (δ) involves neighboring coefficients of the wavelet decomposition for the estimation of the local variance. Weighted variance (δ) of a given wavelet coefficient is determined by the weight in a local window.

$$\delta = \frac{\sum_{i,j \in N} w_{i,j} Y[x,y]^2}{\sum_{i,j \in N} w_{i,j}}$$

22

$Y[x,y]$ is pixel value of the image. w is the weight of the local window. The selection of weights for the calculation of weighted variance would be in such a way that the estimated threshold minimizes the Mean square error.

Threshold (λ) is calculate from noise variance(σ) by weighted variance(δ).

$$\lambda(x, y) = \sigma(x, y) / \delta(x, y)$$

The parameter noise variance (σ) needs to be estimated. It may be possible to measure (σ) based on information other than the corrupted image and it is estimated from the sub band HH by the robust median estimator,

$$\sigma^2(x, y) = [\text{median}/0.6745]^2$$

where 0.6745 is the experimental value.

For quantitative analysis parameters MSE (Mean Square Error), PSNR (peak signal to noise ratio) are calculated for all the standard images with their noisy and denoised counterparts,

$$\text{PSNR} = 10 \log_{10} (255^2 / \text{MSE})$$

$$\text{MSE} = 1 / (M \times N) \sum [X(i,j) - Y(i,j)]^2$$

where X and Y are the original and noisy or denoised image respectively. M and N represent the width and height of image.

23

CHAPTER 6 SIMULATION RESULTS

A program is written and implemented in matlab for denoising the ultrasound images.

MATLAB (matrix laboratory) is a numerical computing environment and fourth-generation programming language. Developed by MathWorks, MATLAB allows matrix manipulations, plotting of functions and data, implementation of algorithms, creation of user interfaces, and interfacing with programs written in other languages, including C, C++, Java, and Fortran.

Key Features

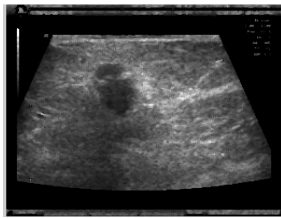
- High-level language for technical computing
- Development environment for managing code, files, and data
- Interactive tools for iterative exploration, design, and problem solving
- Mathematical functions for linear algebra, statistics, Fourier analysis, filtering, optimization, and numerical integration
- 2-D and 3-D graphics functions for visualizing data

The resulting images at various stages of the algorithm for the given input image are shown and attached here.

24



(a) Input Noisy Image



(b) Denoised Image by Median Filter



(c) Denoised Image by Lee Filter



(d) Denoised Image by Kaun Filter



(e) Denoised Image by SRAD



(f) Denoised Image by Wavelet (Haar)



(g) Denoised Image by Wavelet (db2)



(h) Denoised Image by Wavelet (db3)

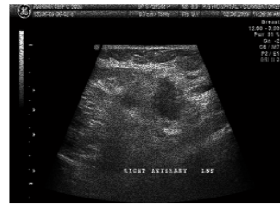


(i) Denoised Image by Wavelet (db4)



(j) Denoised Image by Wavelet (db5)

Figure 6.1 Simulation Results for Breast Image



(a) Input Noisy Image



(b) Denoised Image by Median Filter



(c) Denoised Image by Lee Filter



(d) Denoised Image by Kaun Filter



(i) Denoised Image by Wavelet (db4)



(j) Denoised Image by Wavelet (db5)

Figure 6.2 Simulation Results for Axillary Image



(e) Denoised Image by SRAD



(f) Denoised Image by Wavelet (Haar)



(a) Input Noisy Image



(b) Denoised Image by Median Filter



(g) Denoised Image by Wavelet (db2)



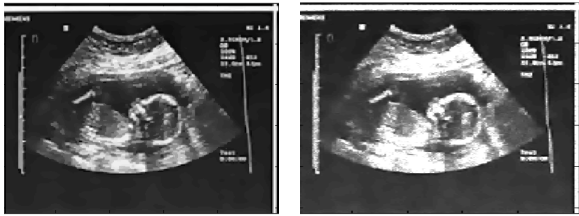
(h) Denoised Image by Wavelet (db3)



(c) Denoised Image by Lee Filter



(d) Denoised Image by Kaun Filter



(e) Denoised Image by SRAD



(f) Denoised Image by Wavelet (Haar)



(g) Denoised Image by Wavelet (db2)



(h) Denoised Image by Wavelet (db3)



(i) Denoised Image by Wavelet (db4)



(j) Denoised Image by Wavelet (db5)

Figure 6.3 Simulation Results for Fetus Image



(a) Input Noisy Image



(b) Denoised Image by Median Filter



(c) Denoised Image by Lee Filter



(d) Denoised Image by Kaun Filter



(e) Denoised Image by SRAD



(f) Denoised Image by Wavelet (Haar)



(g) Denoised Image by Wavelet (db2)



(h) Denoised Image by Wavelet (db3)



(i) Denoised Image by Wavelet (db4)



(j) Denoised Image by Wavelet (db5)

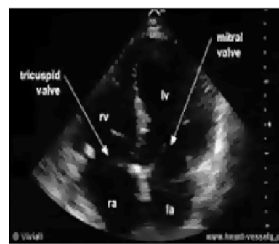
Figure 6.4 Simulation Results for Brain Image



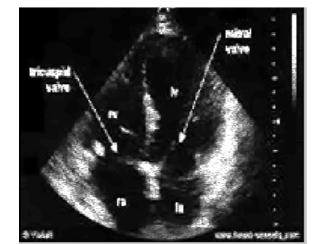
(c) Denoised Image by Lee Filter



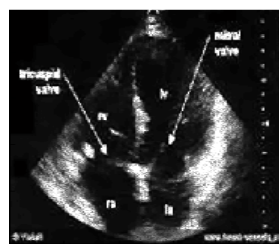
(d) Denoised Image by Kaun Filter



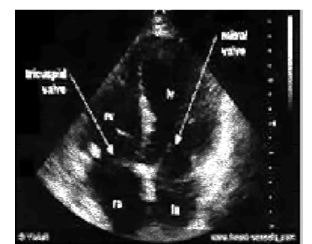
(e) Denoised Image by SRAD



(f) Denoised Image by Wavelet (Haar)



(g) Denoised Image by Wavelet (db2)



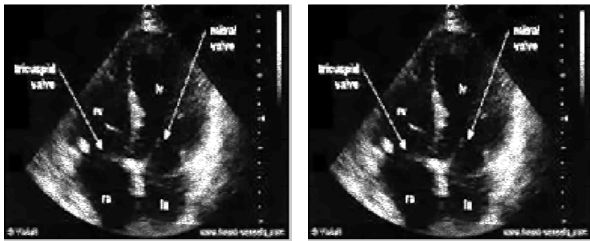
(h) Denoised Image by Wavelet (db3)



(a) Input Noisy Image

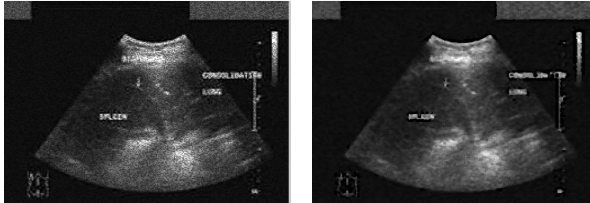


(b) Denoised Image by Median Filter

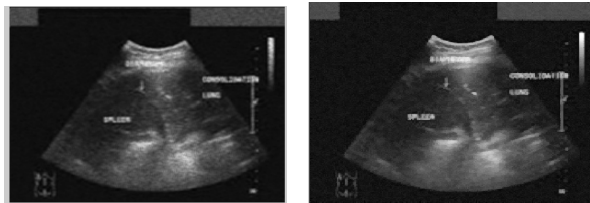


(i) Denoised Image by Wavelet (db4) (j) Denoised Image by Wavelet (db5)

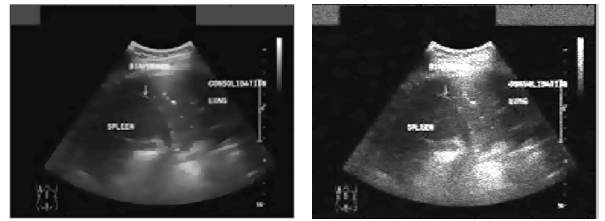
Figure 6.5 Simulation Results for Heart Image



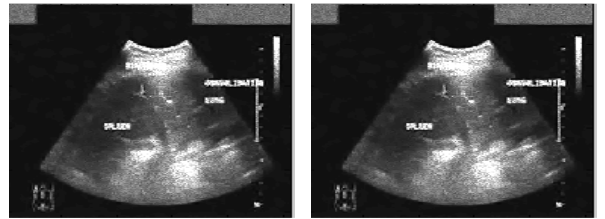
(a) Input Noisy Image (b) Denoised Image by Median Filter



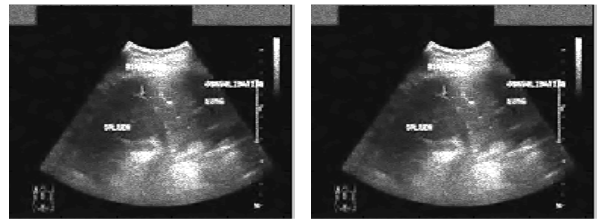
(c) Denoised Image by Lee Filter (d) Denoised Image by Kaun Filter



(e) Denoised Image by SRAD (f) Denoised Image by Wavelet (Haar)



(g) Denoised Image by Wavelet (db2) (h) Denoised Image by Wavelet (db3)



(i) Denoised Image by Wavelet (db4) (j) Denoised Image by Wavelet (db5)

Figure 6.6 Simulation Results for Lungs Image

Table 6.1 PSNR for Breast Image

FILTER	PSNR(db)
MEDIAN	23.7842
LEE	23.6149
KAUN	15.0241
SRAD	23.9094
WAVELET HAAR	24.0654
WAVELET db2	24.0654
WAVELET db3	24.0654
WAVELET db4	24.0654
WAVELET db5	24.0654

Table 6.2 PSNR for Axillary Image

FILTER	PSNR(db)
MEDIAN	23.6949
LEE	23.6063
KAUN	14.9800
SRAD	23.9094
WAVELET HAAR	24.0654
WAVELET db2	24.0654
WAVELET db3	24.0654
WAVELET db4	24.0654
WAVELET db5	24.0654

Table 6.3 PSNR for Fetus Image

FILTER	PSNR(db)
MEDIAN	23.6949
LEE	23.9794
KAUN	14.9792
SRAD	24.0053
WAVELET HAAR	24.0654
WAVELET db2	24.0654
WAVELET db3	24.0654
WAVELET db4	24.0654
WAVELET db5	24.0654

Table 6.4 PSNR for Brain Image

FILTER	PSNR(db)
MEDIAN	23.8445
LEE	23.6922
KAUN	14.9804
SRAD	23.7869
WAVELET HAAR	24.0654
WAVELET db2	24.0654
WAVELET db3	24.0654
WAVELET db4	24.0654
WAVELET db5	24.0654

Table 6.5 PSNR for Heart Image

FILTER	PSNR(db)
MEDIAN	23.7681
LEE	23.9794
KAUN	15.0079
SRAD	24.0042
WAVELET HAAR	24.0654
WAVELET db2	24.0654
WAVELET db3	24.0654
WAVELET db4	24.0654
WAVELET db5	24.0654

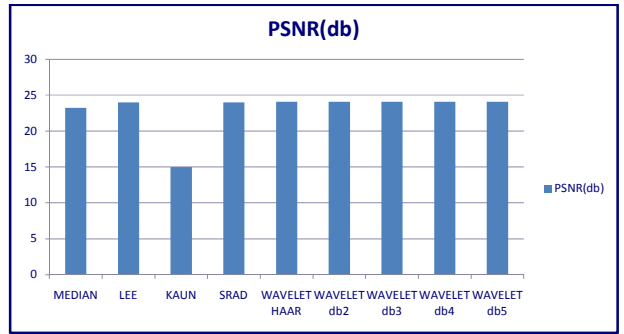


Figure 6.7 PSNR for Breast Image

Table 6.6 PSNR for Lungs Image

FILTER	PSNR(db)
MEDIAN	23.2337
LEE	23.9967
KAUN	14.9883
SRAD	23.9774
WAVELET HAAR	24.0654
WAVELET db2	24.0654
WAVELET db3	24.0654
WAVELET db4	24.0654
WAVELET db5	24.0654

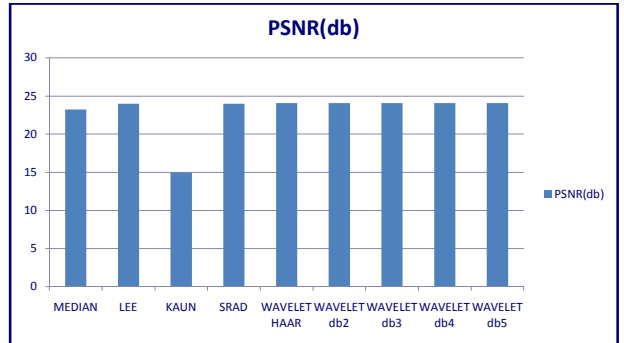


Figure 6.8 PSNR for Axillary Image

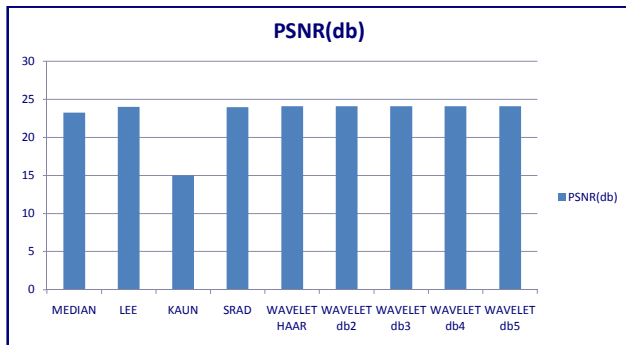


Figure 6.9 PSNR for Fetus Image

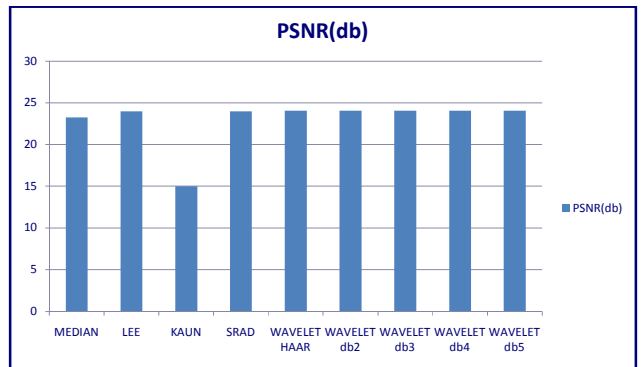


Figure 6.11 PSNR for Heart Image

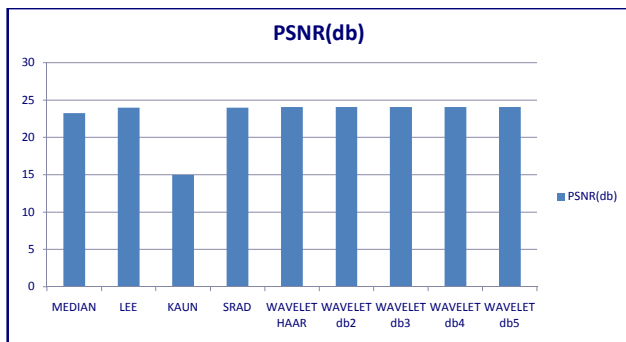


Figure 6.10 PSNR for Brain Image

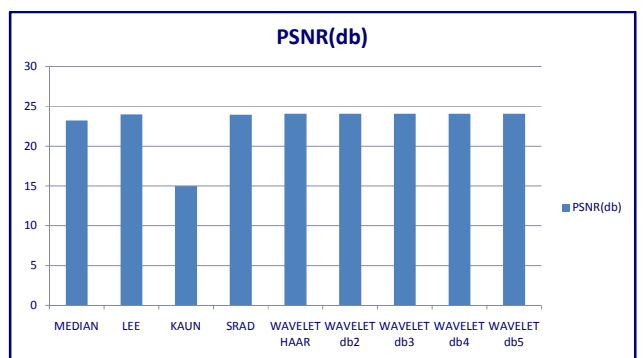


Figure 6.12 PSNR for Lungs Image

Table 6.7 MSE for Breast Image

WAVELET	MSE
HAAR	3.6224
db2	3.5712
db3	3.5674
db4	3.4503
db5	3.5089

Table 6.8 MSE for Axillary Image

WAVELET	MSE
HAAR	0.0421
db2	0.0377
db3	0.0364
db4	0.0355
db5	0.0367

Table 6.9 MSE for Fetus Image

WAVELET	MSE
HAAR	0.8519
db2	0.8022
db3	0.7830
db4	0.7785
db5	0.7824

Table 6.10 MSE for Brain Image

WAVELET	MSE
HAAR	0.1625
db2	0.1654
db3	0.1650
db4	0.1659
db5	0.1711

Table 6.11 MSE for Heart Image

WAVELET	MSE
HAAR	0.5379
db2	0.5058
db3	0.4937
db4	0.4948
db5	0.5056

Table 6.12 MSE for Lungs Image

WAVELET	MSE
HAAR	0.0604
db2	0.0605
db3	0.0616
db4	0.0618
db5	0.0639

Table 6.13 . Threshold Value

IMAGES	TRESHOLD
Breast	3.0976
Axillary	0.3404
Fetus	1.5032
Brain	0.7304
Heart	1.2194
Lungs	0.4359

CHAPTER 7**CONCLUSION & FUTURE SCOPE****Conclusion**

In this work a relatively simple context-based model has been introduced for adaptive threshold selection within a wavelet thresholding framework. Estimations of local weighted variance with appropriately chosen weights are used to adapt the threshold. The proposed thresholding technique outperforms all the standard speckle filters, Median, Lee, Kaun, SRAD methods. However, by visual inspection it is evident that the denoised image, while removing a substantial amount of noise, suffers practically no degradation in sharpness and details. Experimental results show that our proposed method yields significantly improved visual quality as well as better SNR compared to the other techniques in the denoising Techniques.

Future Scope

Multi wavelet may be used to improve the PSNR

CHAPTER 8**BIBLIOGRAPHY**

- [1] Jappret Kaur, Jasdeep Kaur and Manpreet Kaur, "Survey of Despeckling techniques for Medical Ultrasound images", International Journal of Computer Theory and Engineering, Vol 2 (4), 1003-1007, 2011.
- [2] S. Sudha, G.R Suresh and R. Suknesh, "Speckle Noise Reduction in Ultrasound images By Wavelet Thresholding Based On Weighted Variance", International Journal of Computer Theory and Engineering, Vol. 1, No. 1, PP 7-12, 2009.
- [3] S. Sudha, G.R Suresh and R. Suknesh, "Speckle Noise Reduction In ultrasound Images Using Context-Based Adaptive Wavelet Thresholding", IETE Journal of Research Vol 55 (issue 3), 2009.
- [4] Nicolae, M.C., Moraru L., Gogu A., Speckle noise reduction of ultrasound images, Medical Ultrasonography an International Journal of Clinical Imaging, Supplement, 11, 2009, 50-51.
- [5] B. Zhang, J. M. Fadili, and J.-L. Starck "Wavelets, Ridgelets and Curvelets for Poisson Noise Removal" IEEE Transactions on Image Processing, 2007.
- [6] Karl Krissian and Carl Fedrjij "Oriented Speckle reducing anisotropic diffusion", IEEE Trans. Image processing, vol.15, no.5 pp.2694-27014, may 2007
- [7] S.G. Chang, Y. Bin and M. Vetterli: 'Adaptive wavelet thresholding for image denoising and compression', IEEE Trans. On Image Processing, vol.9, no.9, pp. 1532-1546, Sep 2006.
- [8] Yuan Chen, Amar Raheja, "Wavelet Lifting For Speckle Noise Reduction In Ultrasound Images", on Vol.3, pp. 3129- 3132, 17-18, Jan. 2006.

[9] S.Aja-fernandez and C.alberola-lopez,"On the estimation of coefficient of variation for anisotropic diffusion speckle filtering", IEEE Trans. Image processing, vol.15, no.9 pp.2694-27014,Sep.2005

[10] J. S. Lee, "Digital image enhancement and noise filtering by use of local statistics," IEEE Trans.

[11] D. T. Kuan, A. A. Sawchuk, T. C. Strand, and P. Chavel, "Adaptive noise smoothing filter for images with signal-dependent noise," IEEE Trans.



**SPECKLE NOISE REDUCTION IN ULTRASOUND IMAGE BY
WAVELET THRESHOLDING**

by
TAMILARASAN,P
Reg. No. 1020106018

of

KUMARAGURU COLLEGE OF TECHNOLOGY

(An Autonomous Institution affiliated to Anna University of Technology, Coimbatore)

COIMBATORE - 641049

A PROJECT REPORT

Submitted to the

**FACULTY OF ELECTRONICS AND COMMUNICATION
ENGINEERING**

*In partial fulfillment of the requirements
for the award of the degree*

of

MASTER OF ENGINEERING

in

APPLIED ELECTRONICS

APRIL 2012

BONAFIDE CERTIFICATE

Certified that this project report entitled “**SPECKLE NOISE REDUCTION IN ULTRASOUND IMAGE BY WAVELET THRESHOLDING**” is the bonafide work of **Mr.Tamilarasan,P [Reg. no.1020106018]** who carried out the research under my supervision. Certified further, that to the best of my knowledge the work reported herein does not form part of any other project or dissertation on the basis of which a degree or award was conferred on an earlier occasion on this or any other candidate.

Project Guide

Ms.S.Sasikala

Head of the Department

Dr. Rajeswari Mariappan

The candidate with university Register no. 1020106018 is examined by us in the project viva-voce examination held on

Internal Examiner

External Examiner

ii

ACKNOWLEDGEMENT

First I would like to express my praise and gratitude to the Lord, who has showered his grace and blessing enabling me to complete this project in an excellent manner. He has made all things beautiful in his time.

I express my sincere thanks to our beloved Director **Dr.J.Shanmugam**, Kumaraguru College of Technology, I thank for his kind support and for providing necessary facilities to carry out the work.

I express my sincere thanks to our beloved Principal **Dr.S.Ramachandran**, Kumaraguru College of Technology, who encouraged me in each and every steps of the project work.

I would like to express my sincere thanks and deep sense of gratitude to our HOD, **Dr.Rajeswari Mariappan**, Department of Electronics and Communication Engineering, for her valuable suggestions and encouragement which paved way for the successful completion of the project work. I also thank her for her kind support and for providing necessary facilities to carry out the work.

In particular, I wish to thank and everlasting gratitude to the project coordinator **Ms.R.Hemalatha, M.E.**, Assistant Professor(SRG), Department of Electronics and Communication Engineering for her expert counseling and guidance to make this project to a great deal of success.

I am greatly privileged to express my deep sense of gratitude to my guide **Ms.S.Sasikala, M.Tech.(Ph.d)**, Associate Professor, Department of Electronics and Communication Engineering, Kumaraguru College of Technology throughout the course of this project work and I wish to convey my deep sense of gratitude to all the teaching and non-teaching of ECE Department for their help and cooperation.

Finally, I thank my parents and my family members for giving me the moral support and abundant blessings in all of my activities and my dear friends who helped me to endure my difficult times with their unflinching support and warm wishes.

iii

ABSTRACT

In medical image processing, image denoising has become a very essential exercise all through the diagnose. Arbitration between the perpetuation of useful diagnostic information and noise suppression must be treasured in medical images. In general we rely on the intervention of a proficient to control the quality of processed images. In certain cases, for instance in Ultrasound images, the noise can restrain information which is valuable for the general practitioner. Consequently medical images are very inconsistent, and it is crucial to operate case to case. This project presents a wavelet-based thresholding scheme for noise suppression in ultrasound images. Quantitative and qualitative comparisons of the results obtained by the proposed method with the results achieved from the other speckle noise reduction techniques demonstrate its higher performance for speckle reduction.

iv

TABLE OF CONTENT

CHAPTER NO	TITLE	PAGE NO	CHAPTER NO	TITLE	PAGE NO
	ABSTRACT	iv	5	WAVELET FILTERING	19
	LIST OF FIGURES	vii		5.1 Wavelet Thresholding	21
	LIST OF TABLES	viii	6	SIMULATION RESULTS	24
1	INTRODUCTION	1	7	CONCLUSION&FUTURE SCOPE	43
	1.1 Project Goal	1	8	BIBLIOGRAPHY	44
	1.2 Software Used	1			
	1.3 Organization Of The Report	2			
2	ULTRASOUND IMAGING SYSTEM	3			
	2.1 Importance Of Ultrasound Image	4			
	2.2 Speckle Noise In Ultrasound Image	5			
3	DESPECKLING FILTERS	6			
	3.1 Filtering Techniques	6			
	3.1.1 Median Filter	6			
	3.1.2 LEE Filter	7			
	3.1.3 Kaun Filter	8			
	3.1.4 SRAD	8			
4	WAVELET	13			
	4.1 Wavelet Definition	13			
	4.1.1 Scaling Filter	13			
	4.1.2 Scaling Function	13			
	4.2 Wavelet Theory	13			
	4.3 Wavelet Transform	14			

v

vi

LIST OF FIGURES

FIGURE NO	CAPTION	PAGE NO
2.1	Block diagram of Ultrasound Imaging System	3
3.1.1.1	Pixel value of image	6
3.1.1.2	Pixel value of Image after Median Filtering	7
3.1.2.1	Flow Chart of LEE Algorithm	8
3.1.4.1	Flow Chart of SRAD Algorithm	12
4.5.1	Types of Wavelets	18
5.1	Decomposition of Wavelets	20
5.1.1	Flow Chart of Wavelet Algorithm	21
6.1	Simulation Result for Breast Image	26
6.2	Simulation Result for Axillary Image	28
6.3	Simulation Result for Fetus Image	29
6.4	Simulation Result for Brain Image	31
6.5	Simulation Result for Heart Image	33
6.6	Simulation Result for Lungs Image	34
6.7	PSNR for Breast Image	38
6.8	PSNR for Axillary Image	38
6.9	PSNR for Fetus Image	39
6.10	PSNR for Brain Image	39
6.11	PSNR for Heart Image	40
6.12	PSNR for Lungs Image	40

vii

LIST OF TABLES

FIGURE NO	CAPTION	PAGE NO
4.5.1	Types Of Wavelets	17
6.1	PSNR for Breast Image	35
6.2	PSNR for Axillary Image	35
6.3	PSNR for Fetus Image	36
6.4	PSNR for Brain Image	36
6.5	PSNR for Heart Image	37
6.6	PSNR for Lungs Image	37
6.7	MSE for Breast Image	41
6.8	MSE for Axillary Image	41
6.9	MSE for Fetus Image	41
6.10	MSE for Brain Image	41
6.11	MSE for Heart Image	41
6.12	MSE for Lungs Image	41
6.13	Threshold Value	42

viii

CHAPTER 1

INTRODUCTION

For the past twenty years, new medical imaging techniques have been under development that image the solid mechanical properties of tissues using pre-existing imaging modalities. An imaging technique involves exposing the object to a form of energy and creating an image from how the object interacts with the input energy. The most popular underlying imaging modality used is ultrasound. Ultrasound imaging is a widely used and safe medical diagnostic technique, due to its noninvasive nature, low cost and capability of forming real time imaging. However the usefulness of ultrasound imaging is degraded by the presence of speckle noise. When structure in the object is too small compared to the wavelength of ultrasound, interference occurs between waves reflected from the object. This produces a mottled appearance in the output image which is termed as speckle noise. The speckle pattern depends on the structure of the image tissue and various imaging parameters. There are two main purposes for speckle reduction in medical ultrasound imaging to improve the human interpretation of ultrasound images and despeckling is the preprocessing step for many ultrasound image processing tasks such as segmentation and registration. A number of methods have been proposed for speckle reduction in ultrasound imaging. While incorporating speckle reduction techniques as an aid for visual diagnosis, it has to keep in mind that certain speckle contains diagnostic information and should be retained. Wavelet based techniques has been used for speckle noise reduction. The results obtained by the wavelets based techniques are compared with other speckle noise reduction techniques to demonstrate its higher performance for speckle noise reduction.

1.1. PROJECT GOAL

The purpose of this project is to reduce speckle noise without losing its significant information in ultrasound images in an efficient way in order to improve the diagnosis.

1.2 SOFTWARES USED

MATLAB R2009a

1

1.3 ORGANIZATION OF THE REPORT

- ✓ Chapter 2 Ultrasound Imaging System.
- ✓ Chapter 3 Despeckling Filters
- ✓ Chapter 4 Wavelets
- ✓ Chapter 5 Wavelet Filtering
- ✓ Chapter 6 Simulation Result
- ✓ Chapter 7 Conclusion
- ✓ Chapter 8 Bibliography

2

CHAPTER 2

ULTRASOUND IMAGING SYSTEM

The construction of ultrasound B-mode image involves capturing the echo signal returned from tissue at the surface of piezoelectric crystal transducers. These transducers convert the ultrasonic RF mechanical wave into electrical signal. Convex ultrasound probes collect the echo from tissue in a radial form. Each group of transducers is simultaneously activated to look at a certain spatial direction from which they generate a raw line signal (stick) to be used later for raster image construction. These sticks are then demodulated and logarithmically compressed to reduce their dynamic range to suit the commercial display devices. The final Cartesian image is constructed from the sampled sticks in a process called scan conversion.

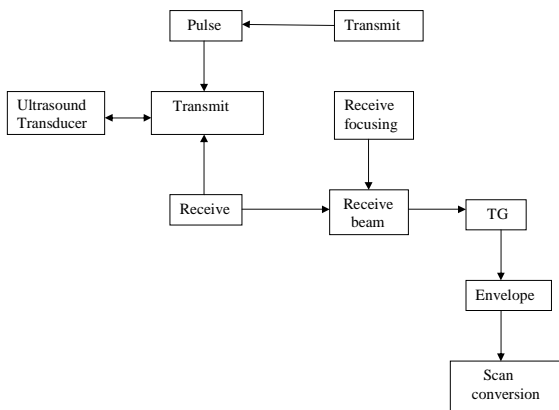


Figure 2.1 Block diagram of Ultrasound Imaging System

3

Speckle reduction techniques can be applied on envelope detected data, log compressed data or on scan converted data. However, slightly different results will be produced for each data. In the compression stage some useful information about the imaged object may be deteriorated or even lost. However, any processing which works with envelope detected data has more information at its disposal and preserves more useful information. Compared to processing the scan converted image, envelope detected data has fewer pixels and thus incurs lower computational cost.

For optimum result envelope detected data processing is preferred because some information that lost after the compression stage cannot be recovered by working with log compressed data or the scan converted image. However, the real time speckle reduction methods are applied on the scan converted image, since the scan converted image is always accessible where most commercial ultrasound systems do not output the envelope detected or log compressed data.

2.1 IMPORTANCE OF ULTRASOUND IMAGING

Ultrasound imaging application in medicine and other fields is enormous. It has several advantages over other medical imaging modalities. The use of ultrasound in diagnosis is well established because of its noninvasive nature, low cost, capability of forming real time imaging and continuing improvement in image quality. It is estimated that one out of every four medical diagnostic image studies in the world involves ultrasonic techniques. US waves are characterized by frequency above 20 KHz which is the upper limit of human hearing. In medical US applications, frequencies are used between 500 KHz and 30 MHz B-mode imaging is the most used modality in medical US. An US transducer which is placed onto the patient's skin over the imaged region sends an US pulse which travels along a beam into the tissue. Due to interfaces some of the US energy is reflected back to the transducer which converts it into echo signals. These signals are then sent into amplifiers and signal processing circuits in the imaging machine's hardware to form a 2-D image. Thus, US imaging involves signals which are obtained by coherent summation of echo signals from scatterers in the tissue. In many cases volume quantification is important in assessing the progression of diseases and tracking progression of response to treatment.

4

Ultrasound-based diagnostic medical imaging technique used to visualize muscles and many internal organs, their size, structure and any pathological injuries with real time tomographic images. It is also used to visualize a fetus during routine and emergency prenatal care. Obstetric sonography is commonly used during pregnancy. It is one of the most widely used diagnostic tools in modern medicine. The technology is relatively inexpensive and portable, especially when compared with other imaging techniques such as magnetic resonance imaging (MRI) and computed tomography (CT). It has no known long-term side effects and rarely causes any discomfort to the patient. Small, easily carried scanners are available examinations can be performed at the bedside. Since it does not use ionizing radiation, ultrasound yields no risks to the patient. It provides live images, where the operator can select the most useful section for diagnosing thus facilitating quick diagnoses. This work aims to suppress speckle in Ultrasound images.

Speckle noise affects all coherent imaging systems including medical ultrasound. Within each resolution cell a number of elementary scatterers reflect the incident wave towards the sensor. The backscattered coherent waves with different phases undergo a constructive or a destructive interference in a random manner. The acquired image is thus corrupted by a random granular pattern, called speckle that delays the interpretation of the image content. A speckled image is commonly modeled as

$$v_i = f_i \xi_i$$

where

$f = \{f_1, f_2, f_3, \dots, f_n\}$ is a noise-free ideal image,

$V = \{v_1, v_2, v_3, \dots, v_n\}$ speckle noise and

$\xi = \{\xi_1, \xi_2, \xi_3, \dots, \xi_n\}$ is a unit mean random field.

The desired grade of speckle smoothing preferably depends on the specialist's knowledge and on the application. For automatic segmentation, sustaining the sharpness of the boundaries between different image regions is usually preferred while smooth out the speckled texture. For visual interpretation, smoothing the texture may be less desirable. Physicians generally have a preference of the original noisy images more willingly than the smoothed versions because the filters even if they are more sophisticated can destroy some relevant image details.

An appropriate method for speckle reduction is one which enhances the signal to noise ratio while preserving the edges and lines in the image. To address the multiplicative nature of speckle noise, Jain developed a homomorphic approach, which is obtained by taking the logarithm of an image, translates the multiplicative noise into additive noise, and consequently applies the Wiener filtering. Recently many techniques have been purposed to reduce the speckle noise using wavelet transform as a multi-resolution image processing tool. Speckle noise is a high-frequency component of the image and appears in wavelet coefficients. One of the widespread method which is mainly exploited for speckle reduction is the wavelet method. A comparative study between wavelet coefficient filter and several standard speckle filters that are being largely used for speckle noise suppression which shows that the wavelet-based approach is deployed among the best for speckle removal.

3.1 FILTERING TECHNIQUES

There are many speckle reduction filters available, some give better visual interpretations while others have good noise reduction or smoothing capabilities. Some of the best known speckle reduction filters are Median, Lee, Kuan and SRAD filters.

3.1.1 MEDIAN FILTER

The Median Filter computes the median of all the pixels within a local window and replaces the center pixel with this median value. Median filtering is a non-linear filtering technique. This method is effective in cases when the noise pattern consists of strong, spike like components and the characteristics to be preserved are edges. The main disadvantage of the median filter is the extra computation time needed to sort the intensity value of each set

15	10	20
23	90	27
33	31	30

Figure 3.1.1.1 Pixel value of image

Sort the pixel value 10 15 20 23 27 30 31 33 90. Find the median 10 15 20 23 27 30 31 33 90

15	10	20
23	27	27
33	31	30

Figure 3.1.1.2 Pixel value of Image after Median Filtering

3.1.2 LEE FILTER

Lee Filter is based on multiplicative speckle model and it can use local statistics to effectively preserve edges. This filter is based on the approach that if the variance over an area is low or constant, then smoothing will not be performed, otherwise smoothing will be performed if variance is high (near edges).

$$Img(i,j) = Im + W * (Cp - Im)$$

Where Img is the pixel Value at indices i, j after filtering, Im is mean intensity of the filter window, Cp is the center pixel and W is a filter window given by:

$$W = \sigma^2 / (\sigma^2 + \rho^2)$$

where σ^2 is the variance of the pixel values within the filter window and is calculated as:

$$\sigma^2 = [1/N \sum_{j=0, N-1} (X_j)^2]$$

Here, N is the size of the filter window and X_j is the pixel value within the filter window at indices j . The parameter ρ is the additive noise variance of the image given in following equation, where M is the size of the image and Y_j is the value of each pixel in the image.

$$\rho^2 = [1/M \sum_{i=0, M-1} (Y_i)^2]$$

If there is no smoothing, the filter will output only the mean intensity value (Im) of the filter window. Otherwise, the difference between Cp and Im is calculated and multiplied with W and then summed with Im . The main drawback of Lee filter is that it tends to ignore speckle noise near edges.

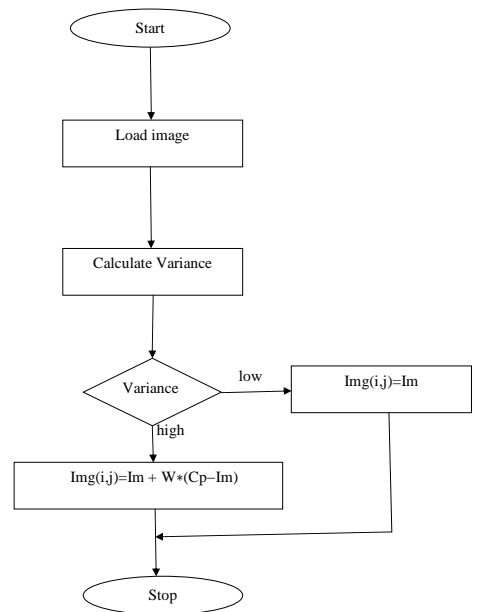


Figure 3.1.2.1 Flow Chart of LEE Algorithm

3.1.3 KAUN FILTER

Kuan filter is a local linear minimum square error filter based on multiplicative order it does not make approximation on the noise variance within the filter window like lee filter it models the multiplicative model of speckle noise into an additive linear form. The weighting function W is computed as follows:

$$W = (1 - Cu/Ci)(1 + Cu)$$

The weighting function is computed from the estimated noise variation coefficient of the image, Cu computed as follows:

$$Cu = \sqrt{1/ENL}$$

And Ci is the variation coefficient of the image computed as follows:

$$Ci = S/Im$$

Where S is the standard deviation in filter window and Im is mean intensity value within the window. The only limitation with Kuan filter is that the ENL parameter is needed for computation.

ENL is Equal Number of Looks which is Calculated as

$$ENL = (\text{Mean Variance}/\text{Standard Deviation})^2$$

3.1.4 SRAD

SRAD stands for Speckle Reduction by Anisotropic Diffusion. In image processing and computer vision, anisotropic diffusion, also called Perona–Malik diffusion, is a technique aiming at reducing image noise without removing significant parts of the image content, typically edges, lines or other details that are important for the interpretation of the image. Anisotropic diffusion resembles the process that creates a scale-space, where an image generates a parameterized family of successively more and more blurred images based on a diffusion process. Each of the

resulting images in this family are given as a convolution between the image and a 2D isotropic Gaussian filter, where the width of the filter increases with the parameter. This diffusion process is a linear and space-invariant transformation of the original image. Anisotropic diffusion is a generalization of this diffusion process: it produces a family of parameterized images, but each resulting image is a combination between the original image and a filter that depends on the local content of the original image. As a consequence, anisotropic diffusion is a non-linear and space-variant transformation of the original image.

In its original formulation, presented by Perona and Malik in 1987, the space-variant filter is in fact isotropic but depends on the image content such that it approximates an impulse function close to edges and other structures that should be preserved in the image over the different levels of the resulting scale-space. This formulation was referred to as anisotropic diffusion by Perona and Malik even though the locally adapted filter is isotropic, but it has also been referred to as inhomogeneous and nonlinear diffusion, or Perona-Malik diffusion. A more general formulation allows the locally adapted filter to be truly anisotropic close to linear structures such as edges or lines: it has an orientation given by the structure such that it is elongated along the structure and narrow across. As a consequence, the resulting images preserve linear structures while at the same time smoothing is made along these structures. Both these cases can be described by a generalization of the usual diffusion equation where the diffusion coefficient, instead of being a constant scalar, is a function of image position and assumes a matrix (or tensor) value.

Although the resulting family of images can be described as a combination between the original image and space-variant filters, the locally adapted filter and its combination with the image do not have to be realized in practice. Anisotropic diffusion is normally implemented by means of an approximation of the generalized diffusion equation: each new image in the family is computed by applying this equation to the previous image. Consequently, anisotropic diffusion is an iterative process where a relatively simple set of computation are used to compute each successive image in the family and this process is continued until a sufficient degree of smoothing is obtained.

SRAD is a Partial Differential Equation (PDE) approach to speckle removal in images. The PDE-based speckle removal approach allows the generation of an image scale space without bias due to filter window size and shape. SRAD is an anisotropic diffusion method for smoothing speckled imagery. Given an intensity image $I_0(x,y)$ having finite power and no zero values over the image support Ω , the output image $I(x, y, t)$ is evolved according to the following PDE:

$$\begin{aligned} \partial I(x,y;t) / \partial t &= \text{div}[c(q)\Delta I(x,y;t)] \\ I(x,y;0) &= I_0(x,y), (\partial I(x,y;t) / \partial n) \partial \Omega = 0 \end{aligned}$$

Where $\partial \Omega$ denotes the border of Ω , n is the outer normal to the $\partial \Omega$, and

$$c(q) = 1 / (1 + q^2(x,y;t) - q_0^2(t) / (q_0^2(t) + q_0^2(t)))$$

$q_0(t)$ is the speckle scale function. In the SRAD, variation $q(x, y, t)$ serves as the edge detector in speckled imagery. The isotropic diffusion in homogenous regions of the image where $q(x, y, t)$ fluctuates around $q_0(t)$. It is estimated using

$$q_0(t) = \text{var}[z(t)] / z(t)$$

where $\text{var}[z(t)]$ and $z(t)$ are the intensity variance and mean over a homogenous area at t , respectively.

3.1.4.1 ALGORITHM

SRAD preserves as well as enhances edges and with the intra region smoothing it reduces speckle noise. In the discrete domain, a gradient can be approximated as the intensity difference between neighboring elements in the image. The filter is iterative $I_0(x,y), (\partial I(x,y;t) / \partial n) \partial \Omega$ describes the change in image intensity produced by one iteration of the filter.

By using the explicit finite difference approach the algorithm for speckle reduction can be designed as the following:

- 1: Design eight 3×3 masks for detecting edges in eight different directions for each pixel of the image.
- 2: for $t = 1$ to n do

- 3: Calculate edges in N,S,E,W,NE,SE,NW,SW directions for each pixel of the image and stored in eight different arrays.
- 4: for all pixels in the image do
- 5: Calculate the value of eight diffusion coefficients for each pixel {Using the elements of the edge arrays}
- 6: Calculate the new intensity of the pixel using the discrete PDE solution.

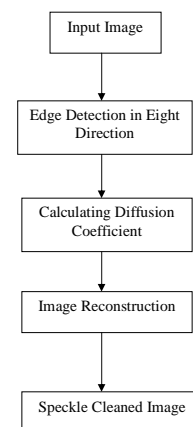


Figure 3.1.4.1 Flow Chart of SRAD Algorithm

CHAPTER 4
WAVELET

4.1 WAVELET DEFINITION

There are a number of ways of defining a wavelet (or a wavelet family).

4.1.1 SCALING FILTER

An orthogonal wavelet is entirely defined by the scaling filter - a low-pass finite impulse response (FIR) filter of length $2N$ and sum 1. In biorthogonal wavelets, separate decomposition and reconstruction filters are defined. For analysis with orthogonal wavelets the high pass filter is calculated as the quadrature mirror filter of the low pass, and reconstruction filters are the time reverse of the decomposition filters. Daubechies and Symlet wavelets can be defined by the scaling filter.

4.1.2 SCALING FUNCTION

Wavelets are defined by the wavelet function $\psi(t)$ (i.e. the mother wavelet) and scaling function $\phi(t)$ (also called father wavelet) in the time domain. The wavelet function is in effect a band-pass filter and scaling it for each level halves its bandwidth. This creates the problem that in order to cover the entire spectrum, an infinite number of levels would be required. The scaling function filters the lowest level of the transform and ensures all the spectrum is covered. For a wavelet with compact support, $\phi(t)$ can be considered finite in length and is equivalent to the scaling filter g . Meyer wavelets can be defined by scaling functions

4.2 WAVELET THEORY

A wavelet is a wave-like oscillation with an amplitude that starts out at zero, increases, and then decreases back to zero. It can typically be visualized as a "brief oscillation" like one might see recorded by a seismograph or heart monitor. Generally, wavelets are purposefully crafted to have specific properties that make them useful for signal processing. Wavelets can be

Wavelet transforms are classified into discrete wavelet transforms (DWTs) and continuous wavelet transforms (CWTs). Note that both DWT and CWT are continuous-time (analog) transforms. They can be used to represent continuous-time (analog) signals. CWTs operate over every possible scale and translation whereas DWTs use a specific subset of scale and translation values or representation grid.

4.3.1 CONTINUOUS WAVELET TRANSFORM

In continuous wavelet transforms, a given signal of finite energy is projected on a continuous family of frequency bands (or similar subspaces of the L^2 function space $L^2(\mathbb{R})$).

For instance the signal may be represented on every frequency band of the form $[f^2, f]$ for all positive frequencies $f > 0$. Then, the original signal can be reconstructed by a suitable integration over all the resulting frequency components.

The frequency bands or subspaces (sub-bands) are scaled versions of a subspace at scale I . This subspace in turn is in most situations generated by the shifts of one generating function $\psi \in L^2(\mathbb{R})$, the mother wavelet. For the example of the scale one frequency band $[1, 2]$ this function is

$$\psi(t) = 2 \operatorname{sinc}(2t) - \operatorname{sinc}(t) = \sin(2\pi t) - \sin(\pi t) / \pi$$

4.3.2 DISCRETE WAVELET TRANSFORM

It is computationally impossible to analyze a signal using all wavelet coefficients, so one may wonder if it is sufficient to pick a discrete subset of the upper half plane to be able to reconstruct a signal from the corresponding wavelet coefficients. One such system is the affine system for some real parameters $a > 1, b > 0$. The corresponding discrete subset of the half plane consists of all the points $(a^m, na^m b)$ with integers $m, n \in \mathbb{Z}$. The corresponding baby wavelets are now given as

$$\psi_{m,n}(t) = a^{-m/2} \psi(a^{-m}t - nb)$$

A sufficient condition for the reconstruction of any signal x of finite energy by the formula

$$x(t) = \sum_{m \in \mathbb{Z}} \sum_{n \in \mathbb{Z}} \langle x, \psi_{m,n} \rangle \psi_{m,n}(t)$$

combined, using a "revert, shift, multiply and sum" technique called convolution, with portions of an unknown signal to extract information from the unknown signal.

A wavelet could be created to have a frequency of Middle C and a short duration of roughly a 32nd note. If this wavelet were to be convolved at periodic intervals with a signal created from the recording of a song, then the results of these convolutions would be useful for determining when the Middle C note was being played in the song. Mathematically, the wavelet will resonate if the unknown signal contains information of similar frequency - just as a tuning fork physically resonates with sound waves of its specific tuning frequency. This concept of resonance is at the core of many practical applications of wavelet theory. As a mathematical tool, wavelets can be used to extract information from many different kinds of data, including - but certainly not limited to - audio signals and images. Sets of wavelets are generally needed to analyze data fully. A set of "complementary" wavelets will deconstruct data without gaps or overlap so that the deconstruction process is mathematically reversible. Thus, sets of complementary wavelets are useful in wavelet based compression/decompression algorithms where it is desirable to recover the original information with minimal loss. In formal terms, this representation is a wavelet series representation of a square-integrable function with respect to either a complete, orthonormal set of basis functions, or an overcomplete set or frame of a vector space, for the Hilbert space of square integrable functions.

4.3 WAVELET TRANSFORM

A wavelet is a mathematical function used to divide a given function or continuous-time signal into different scale components. Usually one can assign a frequency range to each scale component. Each scale component can then be studied with a resolution that matches its scale. A wavelet transform is the representation of a function by wavelets. The wavelets are scaled and translated copies (known as "daughter wavelets") of a finite-length or fast-decaying oscillating waveform (known as the "mother wavelet"). Wavelet transforms have advantages over traditional Fourier transforms for representing functions that have discontinuities and sharp peaks, and for accurately deconstructing and reconstructing finite, non-periodic and/or non-stationary signals.

is that the functions $\psi_{m,n} : m, n \in \mathbb{Z}$ form a tight frame of $L^2(\mathbb{R})$.

4.4 APPLICATION OF WAVELETS

An approximation to DWT is used for data compression if signal is already sampled, and the CWT for signal analysis. Thus, DWT approximation is commonly used in engineering and computer science, and the CWT in scientific research.

Wavelet transforms are now being adopted for a vast number of applications, often replacing the conventional Fourier Transform. Many areas of physics have seen this paradigm shift, including molecular dynamics, ab initio calculations, astrophysics, density matrix localization, seismology, optics, turbulence, and quantum mechanics. This change has also occurred in image processing, blood-pressure, heart-rate, and ECG analyses, brain rhythms, DNA analysis, protein analysis, climatology, general signal processing, speech recognition, computer graphics and multi fractal analysis. In computer vision and image processing, the notion of scale-space representation and Gaussian derivative operators is regarded as a canonical multi-scale representation.

One use of wavelet approximation is in data compression. Like some other transforms, wavelet transforms can be used to transform data, then encode the transformed data, resulting in effective compression. For example, JPEG 2000 is an image compression standard that uses biorthogonal wavelets. This means that although the frame is overcomplete, it is a *tight frame* (see types of Frame of a vector space), and the same frame functions (except for conjugation in the case of complex wavelets) are used for both analysis and synthesis, i.e., in both the forward and inverse transform. For details see wavelet compression.

A related use is for smoothing/denoising data based on wavelet coefficient thresholding, also called wavelet shrinkage. By adaptively thresholding the wavelet coefficients that correspond to undesired frequency components smoothing and/or denoising operations can be performed.

Wavelet transforms are also starting to be used for communication applications. Wavelet OFDM is the basic modulation scheme used in HD-PLC (a power line communications technology developed by Panasonic), and in one of the optional modes included

in the IEEE 1901 standard. Wavelet OFDM can achieve deeper notches than traditional FFT OFDM, and wavelet OFDM does not require a guard interval (which usually represents significant overhead in FFT OFDM systems).

4.5 TYPES OF WAVELETS

Table 4.5.1 Types of Wavelets

Family Name	Short Name
Haar wavelet	'haar'
Daubechies wavelets	'db'
Symlets	'sym'
Coiflets	'coif'
Biorthogonal wavelets	'bior'
Reverse biorthogonal wavelets	'rbio'
Meyer wavelet	'meyr'
Discrete approximation of Meyer wavelet	'dmey'
Gaussian wavelets	'gaus'
Mexican hat wavelet	'mexh'
Morlet wavelet	'morl'
Complex Gaussian wavelets	'cgau'
Shannon wavelets	'shan'
Frequency B-Spline wavelets	'fbsp'
Complex Morlet wavelets	'cmor'

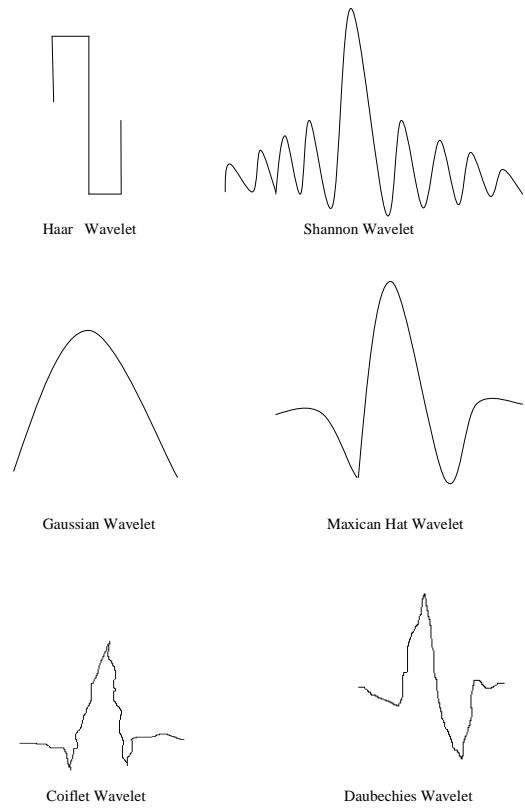


Figure 4.5.1 Types of Wavelets

CHAPTER 5

WAVELET FILTERING

Recently there has been significant investigations in medical imaging area using the wavelet transform as a tool for improving medical images from noisy data. Wavelet denoising attempts to remove the noise present in the signal while preserving the signal characteristics, regardless of its frequency content. As the discrete wavelet transform (DWT) corresponds to basis decomposition, it provides a non redundant and unique representation of the signal.

Several properties of the wavelet transform, which make this representation attractive for denoising, are

- Multiresolution - image details of different sizes are analyzed at the appropriate resolution scales
- Sparsity - the majority of the wavelet coefficients are small in magnitude.
- Edge detection - large wavelet coefficients coincide with image edges.
- Edge clustering - the edge coefficients within each sub band tend to form spatially connected clusters

During a two level of decomposition of an image using a scalar wavelet, the two-dimensional data is replaced with four blocks. These blocks correspond to the sub bands that represent either low pass filtering or high pass filtering in each direction. The procedure for wavelet decomposition consists of consecutive operations on rows and columns of the two-dimensional data. The wavelet transform first performs one step of the transform on all rows. This process yields a matrix where the left side contains down sampled low pass coefficients of each row, and the right side contains the high pass coefficients. Next, one step of decomposition is applied to all columns; this results in four types of coefficients, HH, HL, LH and LL. The HH subband gives the diagonal information of the ultra sound image; the HL subband gives the horizontal features while the LH subband represents the vertical structures of the US image. The LL subband is the low-resolution residual consisting of low frequency components.

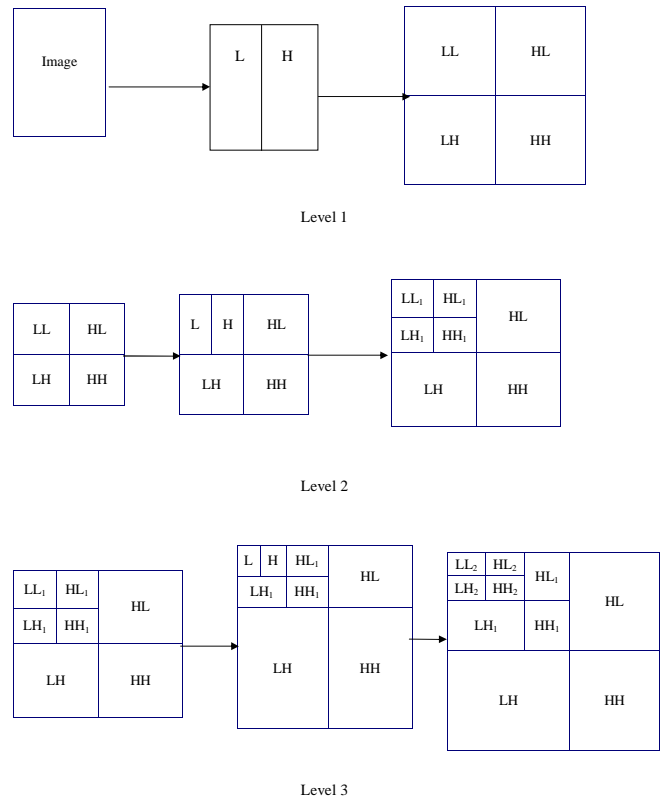


Figure 5.1 Decomposition of Wavelets

5.1 WAVELET THRESHOLDING

All the wavelet filters use wavelet thresholding operation for denoising. Speckle noise is a high-frequency component of the image and appears in wavelet coefficients. One widespread method exploited for speckle reduction is wavelet thresholding procedure. The basic Procedure for all thresholding method is as follows:

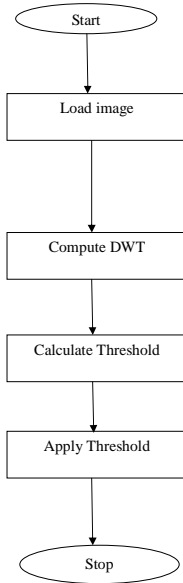


Figure 5.1.1 Flow Chart of Algorithm

21

This section depicts the image-denoising algorithm, which achieves near optimal soft thresholding in the wavelet domain for recovering original signal from the noisy one. The wavelet transform employs Daubechies' least asymmetric compactly supported wavelet with eight vanishing moments with four scales of orthogonal decomposition. It has the following steps.

Transform the multiplicative noise model into an additive one by taking the logarithm of the original speckled data.

- $\text{Log } I(x, y) = \log S(x, y) + \log \eta(x, y)$.
- Perform the DWT of the noisy image
- Obtain noise variance.
- Calculate the weighted variance of image.
- Compute the threshold value for each pixel.
- Perform the inverse DWT to reconstruct the denoised image.
- Take Exponent.

In general a small threshold value will leave behind all the noisy coefficients and subsequently the resultant denoised image may still being noisy. On the other hand a large threshold value makes more number of coefficients as zero which directs to smooth the signal destroys details and the resultant image may cause blur and artifacts. So optimum threshold value should be found out, which is adaptive to different sub band characteristics. Thus the innovative aspects of the present work consist of the estimating appropriate threshold by analyzing the statistical parameters of the wavelet coefficients. Our threshold is based on Universal thresholding function. Threshold is calculated by estimating a parameter weighted variance (δ). The parameter weighted variance (δ) involves neighboring coefficients of the wavelet decomposition for the estimation of the local variance. Weighted variance (δ) of a given wavelet coefficient is determined by the weight in a local window.

$$\delta = \frac{\sum_{i,j \in N} w_{i,j} Y[x,y]^2}{\sum_{i,j \in N} w_{i,j}}$$

22

$Y[x,y]$ is pixel value of the image. w is the weight of the local window. The selection of weights for the calculation of weighted variance would be in such a way that the estimated threshold minimizes the Mean square error.

Threshold (λ) is calculate from noise variance(σ) by weighted variance(δ).

$$\lambda(x, y) = \sigma(x, y) / \delta(x, y)$$

The parameter noise variance (σ) needs to be estimated. It may be possible to measure (σ) based on information other than the corrupted image and it is estimated from the sub band HH by the robust median estimator,

$$\sigma^2(x, y) = [\text{median}/0.6745]^2$$

where 0.6745 is the experimental value.

For quantitative analysis parameters MSE (Mean Square Error), PSNR (peak signal to noise ratio) are calculated for all the standard images with their noisy and denoised counterparts,

$$\text{PSNR} = 10 \log_{10} (255^2 / \text{MSE})$$

$$\text{MSE} = 1 / (M \times N) \sum [X(i,j) - Y(i,j)]^2$$

where X and Y are the original and noisy or denoised image respectively. M and N represent the width and height of image.

23

CHAPTER 6 SIMULATION RESULTS

A program is written and implemented in matlab for denoising the ultrasound images.

MATLAB (matrix laboratory) is a numerical computing environment and fourth-generation programming language. Developed by MathWorks, MATLAB allows matrix manipulations, plotting of functions and data, implementation of algorithms, creation of user interfaces, and interfacing with programs written in other languages, including C, C++, Java, and Fortran.

Key Features

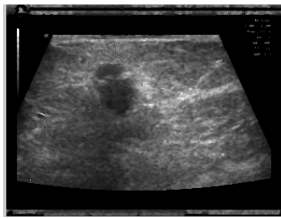
- High-level language for technical computing
- Development environment for managing code, files, and data
- Interactive tools for iterative exploration, design, and problem solving
- Mathematical functions for linear algebra, statistics, Fourier analysis, filtering, optimization, and numerical integration
- 2-D and 3-D graphics functions for visualizing data

The resulting images at various stages of the algorithm for the given input image are shown and attached here.

24



(a) Input Noisy Image



(b) Denoised Image by Median Filter



(c) Denoised Image by Lee Filter



(d) Denoised Image by Kaun Filter



(e) Denoised Image by SRAD



(f) Denoised Image by Wavelet (Haar)



(g) Denoised Image by Wavelet (db2)



(h) Denoised Image by Wavelet (db3)

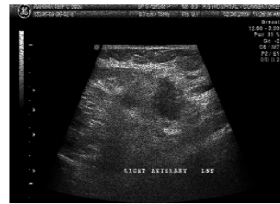


(i) Denoised Image by Wavelet (db4)



(j) Denoised Image by Wavelet (db5)

Figure 6.1 Simulation Results for Breast Image



(a) Input Noisy Image



(b) Denoised Image by Median Filter



(c) Denoised Image by Lee Filter



(d) Denoised Image by Kaun Filter



(i) Denoised Image by Wavelet (db4)



(j) Denoised Image by Wavelet (db5)

Figure 6.2 Simulation Results for Axillary Image



(e) Denoised Image by SRAD



(f) Denoised Image by Wavelet (Haar)



(a) Input Noisy Image



(b) Denoised Image by Median Filter



(g) Denoised Image by Wavelet (db2)



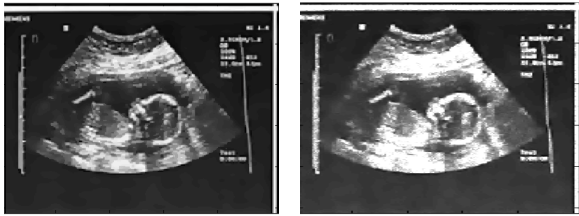
(h) Denoised Image by Wavelet (db3)



(c) Denoised Image by Lee Filter



(d) Denoised Image by Kaun Filter



(e) Denoised Image by SRAD



(f) Denoised Image by Wavelet (Haar)



(g) Denoised Image by Wavelet (db2)



(h) Denoised Image by Wavelet (db3)



(i) Denoised Image by Wavelet (db4)



(j) Denoised Image by Wavelet (db5)

Figure 6.3 Simulation Results for Fetus Image



(a) Input Noisy Image



(b) Denoised Image by Median Filter



(c) Denoised Image by Lee Filter



(d) Denoised Image by Kaun Filter



(e) Denoised Image by SRAD



(f) Denoised Image by Wavelet (Haar)



(g) Denoised Image by Wavelet (db2)



(h) Denoised Image by Wavelet (db3)



(i) Denoised Image by Wavelet (db4)



(j) Denoised Image by Wavelet (db5)

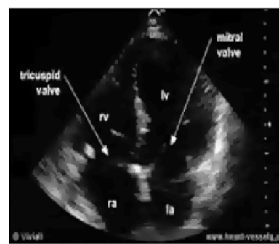
Figure 6.4 Simulation Results for Brain Image



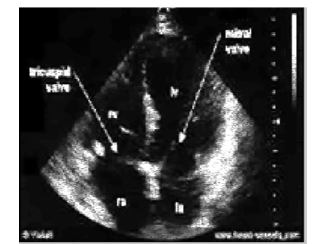
(c) Denoised Image by Lee Filter



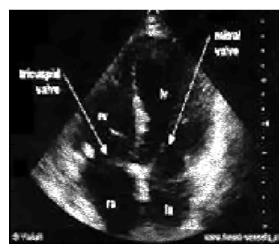
(d) Denoised Image by Kaun Filter



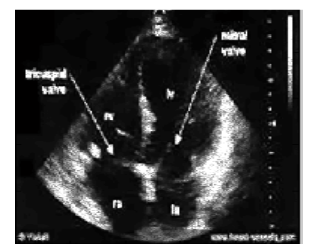
(e) Denoised Image by SRAD



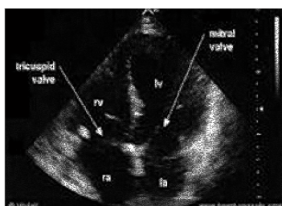
(f) Denoised Image by Wavelet (Haar)



(g) Denoised Image by Wavelet (db2)



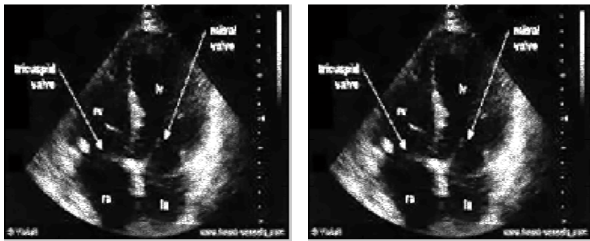
(h) Denoised Image by Wavelet (db3)



(a) Input Noisy Image

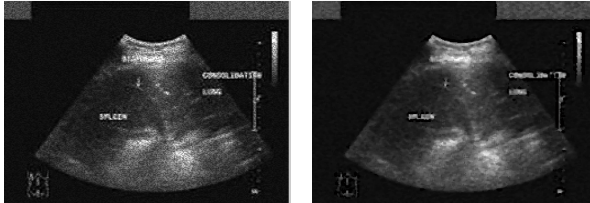


(b) Denoised Image by Median Filter

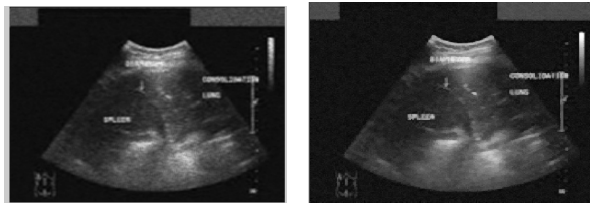


(i) Denoised Image by Wavelet (db4) (j) Denoised Image by Wavelet (db5)

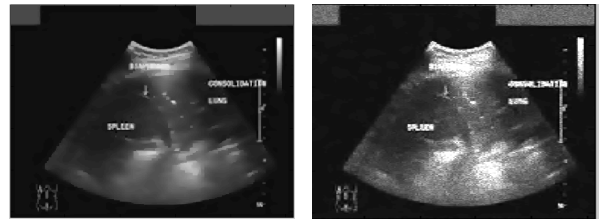
Figure 6.5 Simulation Results for Heart Image



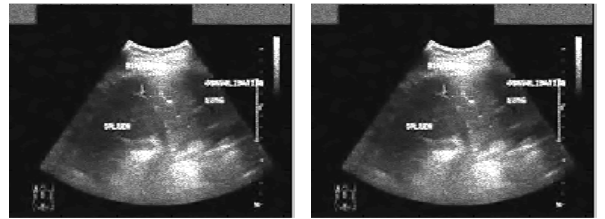
(a) Input Noisy Image (b) Denoised Image by Median Filter



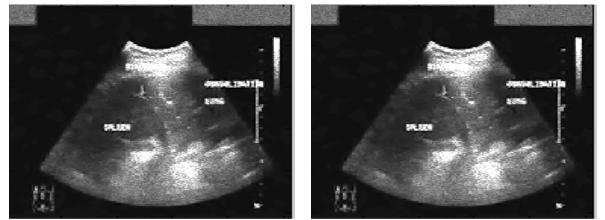
(c) Denoised Image by Lee Filter (d) Denoised Image by Kaun Filter



(e) Denoised Image by SRAD (f) Denoised Image by Wavelet (Haar)



(g) Denoised Image by Wavelet (db2) (h) Denoised Image by Wavelet (db3)



(i) Denoised Image by Wavelet (db4) (j) Denoised Image by Wavelet (db5)

Figure 6.6 Simulation Results for Lungs Image

Table 6.1 PSNR for Breast Image

FILTER	PSNR(db)
MEDIAN	23.7842
LEE	23.6149
KAUN	15.0241
SRAD	23.9094
WAVELET HAAR	24.0654
WAVELET db2	24.0654
WAVELET db3	24.0654
WAVELET db4	24.0654
WAVELET db5	24.0654

Table 6.2 PSNR for Axillary Image

FILTER	PSNR(db)
MEDIAN	23.6949
LEE	23.6063
KAUN	14.9800
SRAD	23.9094
WAVELET HAAR	24.0654
WAVELET db2	24.0654
WAVELET db3	24.0654
WAVELET db4	24.0654
WAVELET db5	24.0654

Table 6.3 PSNR for Fetus Image

FILTER	PSNR(db)
MEDIAN	23.6949
LEE	23.9794
KAUN	14.9792
SRAD	24.0053
WAVELET HAAR	24.0654
WAVELET db2	24.0654
WAVELET db3	24.0654
WAVELET db4	24.0654
WAVELET db5	24.0654

Table 6.4 PSNR for Brain Image

FILTER	PSNR(db)
MEDIAN	23.8445
LEE	23.6922
KAUN	14.9804
SRAD	23.7869
WAVELET HAAR	24.0654
WAVELET db2	24.0654
WAVELET db3	24.0654
WAVELET db4	24.0654
WAVELET db5	24.0654

Table 6.5 PSNR for Heart Image

FILTER	PSNR(db)
MEDIAN	23.7681
LEE	23.9794
KAUN	15.0079
SRAD	24.0042
WAVELET HAAR	24.0654
WAVELET db2	24.0654
WAVELET db3	24.0654
WAVELET db4	24.0654
WAVELET db5	24.0654

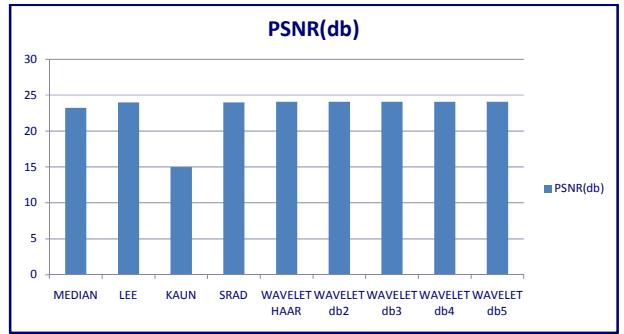


Figure 6.7 PSNR for Breast Image

Table 6.6 PSNR for Lungs Image

FILTER	PSNR(db)
MEDIAN	23.2337
LEE	23.9967
KAUN	14.9883
SRAD	23.9774
WAVELET HAAR	24.0654
WAVELET db2	24.0654
WAVELET db3	24.0654
WAVELET db4	24.0654
WAVELET db5	24.0654

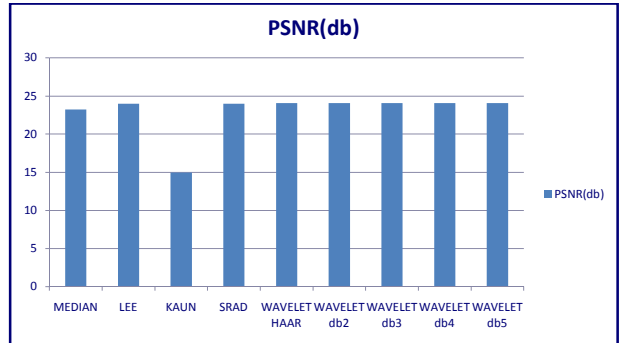


Figure 6.8 PSNR for Axillary Image

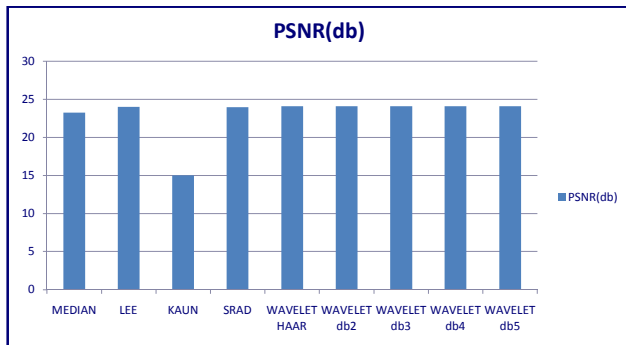


Figure 6.9 PSNR for Fetus Image

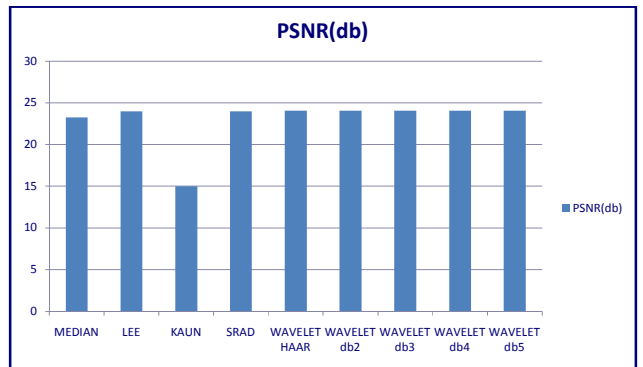


Figure 6.11 PSNR for Heart Image

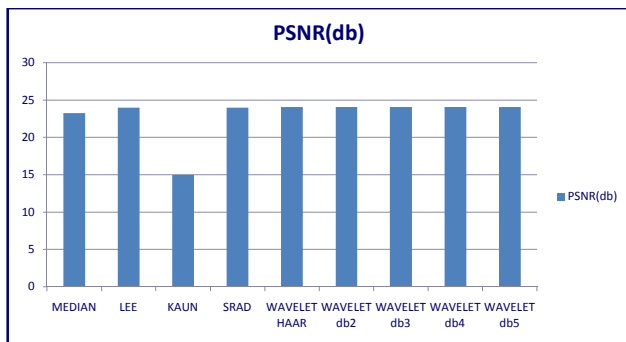


Figure 6.10 PSNR for Brain Image

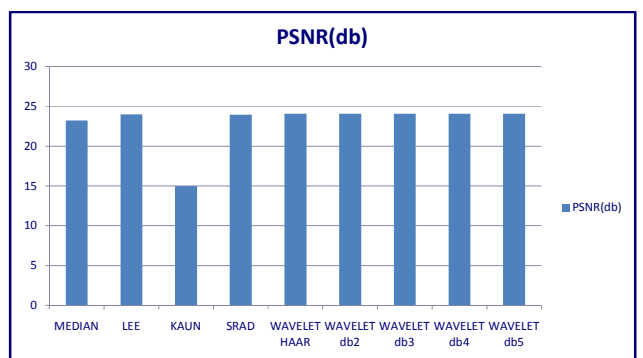


Figure 6.12 PSNR for Lungs Image

Table 6.7 MSE for Breast Image

WAVELET	MSE
HAAR	3.6224
db2	3.5712
db3	3.5674
db4	3.4503
db5	3.5089

Table 6.8 7 MSE for Axillary Image

WAVELET	MSE
HAAR	0.0421
db2	0.0377
db3	0.0364
db4	0.0355
db5	0.0367

Table 6.9 7 MSE for Fetus Image

WAVELET	MSE
HAAR	0.8519
db2	0.8022
db3	0.7830
db4	0.7785
db5	0.7824

Table 6.10 7 MSE for Brain Image

WAVELET	MSE
HAAR	0.1625
db2	0.1654
db3	0.1650
db4	0.1659
db5	0.1711

Table 6.11 7 MSE for Heart Image

WAVELET	MSE
HAAR	0.5379
db2	0.5058
db3	0.4937
db4	0.4948
db5	0.5056

Table 6.12 7 MSE for Lungs Image

WAVELET	MSE
HAAR	0.0604
db2	0.0605
db3	0.0616
db4	0.0618
db5	0.0639

Table 6.13 . Threshold Value

IMAGES	TRESHOLD
Breast	3.0976
Axillary	0.3404
Fetus	1.5032
Brain	0.7304
Heart	1.2194
Lungs	0.4359

CHAPTER 7**CONCLUSION & FUTURE SCOPE****Conclusion**

In this work a relatively simple context-based model has been introduced for adaptive threshold selection within a wavelet thresholding framework. Estimations of local weighted variance with appropriately chosen weights are used to adapt the threshold. The proposed thresholding technique outperforms all the standard speckle filters, Median, Lee, Kaun, SRAD methods. However, by visual inspection it is evident that the denoised image, while removing a substantial amount of noise, suffers practically no degradation in sharpness and details. Experimental results show that our proposed method yields significantly improved visual quality as well as better SNR compared to the other techniques in the denoising Techniques.

Future Scope

Multi wavelet may be used to improve the PSNR

CHAPTER 8**BIBLIOGRAPHY**

- [1] Jappret Kaur, Jasdeep Kaur and Manpreet Kaur, "Survey of Despeckling techniques for Medical Ultrasound images", International Journal of Computer Theory and Engineering, Vol 2 (4), 1003-1007, 2011.
- [2] S. Sudha, G.R Suresh and R. Suknesh, "Speckle Noise Reduction in Ultrasound images By Wavelet Thresholding Based On Weighted Variance", International Journal of Computer Theory and Engineering, Vol. 1, No. 1, PP 7-12, 2009.
- [3] S. Sudha, G.R Suresh and R. Suknesh, "Speckle Noise Reduction In ultrasound Images Using Context-Based Adaptive Wavelet Thresholding", IETE Journal of Research Vol 55 (issue 3), 2009.
- [4] Nicolae, M.C., Moraru L., Gogu A., Speckle noise reduction of ultrasound images, Medical Ultrasonography an International Journal of Clinical Imaging, Supplement, 11, 2009, 50-51.
- [5] B. Zhang, J. M. Fadili, and J.-L. Starck "Wavelets, Ridgelets and Curvelets for Poisson Noise Removal" IEEE Transactions on Image Processing, 2007.
- [6] Karl Krissian and Carl Fedrjij "Oriented Speckle reducing anisotropic diffusion", IEEE Trans. Image processing, vol.15, no.5 pp.2694-27014, may 2007
- [7] S.G. Chang, Y. Bin and M. Vetterli: 'Adaptive wavelet thresholding for image denoising and compression', IEEE Trans. On Image Processing, vol.9, no.9, pp. 1532-1546, Sep 2006.
- [8] Yuan Chen, Amar Raheja, "Wavelet Lifting For Speckle Noise Reduction In Ultrasound Images", on Vol.3, pp. 3129- 3132, 17-18, Jan. 2006.

[9] S.Aja-fernandez and C.alberola-lopez,"On the estimation of coefficient of variation for anisotropic diffusion speckle filtering", IEEE Trans. Image processing, vol.15, no.9 pp.2694-27014,Sep.2005

[10] J. S. Lee, "Digital image enhancement and noise filtering by use of local statistics," IEEE Trans.

[11] D. T. Kuan, A. A. Sawchuk, T. C. Strand, and P. Chavel, "Adaptive noise smoothing filter for images with signal-dependent noise," IEEE Trans.